Analysis of different Supercritical CO_2 Brayton Cycles Integrated with Transcritical CO_2 Cycle and Organic Rankine Cycle

Submitted By

Khandekar Nazmus Sadat

180011121

Supervised By

Dr. Mohammad Monjurul Ehsan

A Thesis submitted in partial fulfilment of the requirement for the degree of Bachelor of Science in Mechanical Engineering

Department of Mechanical and Production Engineering (MPE)

Islamic University of Technology (IUT)

21 June, 2023

Candidate's Declaration

This is to certify that the work presented in this thesis, titled, **Analysis of different Supercritical CO_2 Brayton Cycles Integrated with Transcritical CO_2 Cycle and Organic Rankine Cycle** is the outcome of the investigation and research carried out by me under the supervision of **Dr**. **Mohammad Monjurul Ehsan**

It is also declared that neither this thesis nor any part of it has been submitted elsewhere for the award of any degree or diploma.

Name of the Student
Student No: 180011121

RECOMMENDATION OF THE BOARD OF SUPERVISORS

The thesis titled **Analysis of different Supercritical CO_2 Brayton Cycles Integrated with Transcritical CO_2 Cycle and Organic Rankine Cycle** submitted by **Khandekar Nazmus Sadat** Student No: **180011121** has been accepted as satisfactory in partial fulfilment of the requirements for the degree of B Sc. in Mechanical Engineering on 21 January, 2023

BOARD OF EXAMINERS

1. ----------
   Dr. Mohammad Monjurul Ehsan (Supervisor)
   Associate Professor
   MPE Dept., IUT, Board Bazar, Gazipur-1704, Bangladesh.

2. ----------
   Dr Shamsuddin Ahmed (Examiner)
   Professor
   MPE Dept., IUT, Board Bazar, Gazipur-1704, Bangladesh.

3. ----------
   Muhammad Mahmood Hasan (Examiner)
   Lecturer
   MPE Dept., IUT, Board Bazar, Gazipur-1704, Bangladesh.

Acknowledgement

For this whole thesis work, I am highly grateful to my supervisor Dr. Mohammad Monjurul Ehsan for his guidance, continuous support, patience, and cooperation. Apart from that, I am extremely thankful to my beloved parents for the continuous mental support, motivation, inspiration and prayers that played a vital role throughout this whole thesis work.

Abstract

For concentrating solar power (CSP) applications, supercritical CO_2 (S-CO_2) has the potential to provide greater cycle efficiency than superheated or supercritical steam cycles. The transcritical CO_2 cycle (TCO_2 cycle) performs well in the domain of low-grade waste heat recovery. As an alternative to TCO_2, the organic Rankine cycle (ORC) has been proposed for recovering waste heat. Studies have been carried out integrating SCO_2 Cycle with either ORC or TCO_2. Until now, simple, recompression and partial cooling configuration of SCO_2 cycle has been focused on and a single cycle is used for waste heat. In this research, a thermodynamic study and optimization of combined power cycles having multiple bottoming cycles are being carried out with the objective of enhancing the total thermal efficiency of power cycles. Besides, along with recompression and partial cooling SCO_2 layout, another additional configuration i.e main compression with intercooling is used. In order to examine the behaviour of combined cycles, parametric analysis is performed with respect to some key parameters. And also, comparison between the combined cycle models is done. Analysis is conducted at 25 MPa maximum and 7.5 MPa minimum pressure at 20°C ambient temperature. Results reveal that rise in S-CO_2 cycle maximum temperature enhances combined cycle thermal efficiency. MCIT enhances efficiency up to 40–45°C owing to pseudocritical effects, then decreases. When the TCO_2 cycle's turbine intake pressure increases, the combined cycle's energy efficiency improves, but only up to a point, then starts falling. However, bottoming cycle condensation temperature decreases efficiency. When compared to corresponding standalone cycle, combined cycle configurations demonstrate significantly improved performance. Furthermore, it is found that the main compression with intercooling models gives better performance than the other two proposed models.

Keywords: Supercritical carbon dioxide; Transcritical carbon dioxide; Critical Point; Condensation Temperature; Turbine inlet pressure; parametric analysis

Table of Contents

List of Figures

List of Tables

Nomenclatures and Symbol

Abbreviation	**Meaning**
S-CO_2	Supercritical Carbon Dioxide
T-CO_2	Transcritical Carbon Dioxide
HTR	High Temperature Recuperator
LTR	Low Temperature Recuperator
ORC	Organic Rankine Cycle
CSP	Concentrated Solar Powerplant
RC	Recompression SCO_2 cycle
PC	Partial Cooling SCO_2 cycle
MC	Main Compression SCO_2 cycle

List of symbols:

m	Mass Flow rate, kg/s
h	Enthalpy, kJ/kgK
S	Entropy, kJ /kg
m_t	Mass flow rate of TCO_2 cycle, kg / s
m_o	Mass flow rate of ORC cycle, kg / s
x	Split Ratio
Q_{in}	Heat input
W_{net}	Net Work Output
T_o	Ambient Temperature
X	Exergy
T_r	Temperature inside heater

Greek Symbols:

ε	Recuperator Effectiveness
η	Efficiency of the cycle

List of Subscripts:

S	Supercritical Carbon Dioxide cycle
T	Transcritical Carbon Dioxide cycle
O	Organic Rankine Cycle
0	Ambient condition
s	Ideal process
R	Inside heater
in	Inlet
out	Outlet
dest	Destruction

Chapter 1: Introduction

1.1 Objectives of the Study:

The main objectives behind this study:

- Improve the overall efficiency of Standalone S CO_2 cycle
- Utilize the waste heat of the S-CO_2 cycle
- Develop the exergy efficiency of the cycle
- Minimize exergy destruction
- Optimize the operating and boundary conditions in order to get the best performance

1.2 Background:

The implementation of new technologies has been emphasized by government organizations and policymakers worldwide as a means of resolving extreme high energy demand and also introducing clean and renewable energy resources. In order to decrease the consumption of fossil fuels, significant focus has been drawn for development of specific technologies that can transform solar thermal energy to electricity efficiently[1]. Due to the lack of readily available water supplies, dry cooling is drawing a lot of attention in applications involving concentrated solar power[2], [3]. In modern world, concentrating solar power (CSP) plants normally use materials like steam, oil to transport solar energy to the power block from absorber. Due to their chemical and physical qualities, these working fluids have various constraints. To circumvent these temperature limits, supercritical CO_2 (S-CO_2) is being researched as medium for operating cycle for CSP applications. Due to its applicability to modern nuclear reactors, the supercritical CO_2 Brayton cycle (S-CO_2 cycle) has the potential to be used in nuclear power plants[4]. The S-CO_2 with its favorable thermodynamic properties (lower critical state, higher specific heat and density in the vicinity of the critical condition) provides superior thermal performance in comparison to conventional stream cycles[5], [6] . Besides, due to having superior chemical properties like potential for global warming of 1, zero potential for ozone depletion, noncombustible, noncorrosive, and nonhazardous, S-CO_2 can provide total environmental protection and secure operation [7], [8].

1.3 Evolution of S-CO_2 cycles:

In the 1960s, Angelino and Feher for the first time proposed the notion of the S-CO_2 Brayton Cycle[9], and there have been a number of successful advances in recent years pertaining to this concept, which is mostly concerned with superconducting magneto-optical devices undertaken in the institutions of research. In recent years, several studies on the S-CO_2 cycles have been conducted. Feher is credited with originally proposing a supercritical carbon dioxide (S-CO_2) Brayton cycle (1966). Ishiyama et al. examined the power-generating technologies of the steam turbine cycle, the helium turbine cycle, and the S-CO_2 cycle. They observed that the S-CO_2 cycle demonstrated desirable characteristics for the nuclear fusion reactor system prototype.

The Brayton cycles having closed loop and working fluid supercritical CO_2 (SCO_2) is suggested as advanced power cycle for future generations. This cycle can be widely used in applications like geothermal, nuclear, hydroelectric, clean coal and concentrating solar thermal plant[10] .This cycle has simple layout compared to conventional superheated/supercritical Rankine cycle and comparatively gives much improved thermal efficiency [11]. Because of having higher thermal efficiency than steam at cycle maximum temperatures (500-600°C) and sound performance at extremely high temperatures where steam cannot be used, the SCO_2 power cycle can substantially reduce the overall cost of the solar power plant[12]. Important component of SCO_2 power facilities is the refrigeration system. Another mentionable feature of SCO_2 fluids is the chilling mechanism which is found close to the critical point [13]. This abrupt modulation, nonlinearity of SCO_2 properties poses a design challenge for heat exchangers. This challenge is not to be faced for the fluids having constant properties. Conboy et al.[14] performed experiment using simple Brayton cycle of capacity 20 kW. He investigated the dynamic performance of the cycle components. Ehsan et al. [15] reviewed the applicable Nusselt number and pressure reduction relations for SCO_2 in a circular conduit. Through proper investigation of reheating and intercooling process and their impact to the main cycle, Xu et al. [16] proposed comprehensive design techniques that can be effectively utilized for SCO_2 power cycles having traditional coal-fired power system for supplying input energy. Yamaguchi et al. presented a solar-powered Rankine cycle that generates electricity and heat from S-CO_2. An experimental prototype showed 25% power generation and heat recovery efficiency.

1.4 Superiority of the Supercritical CO_2 cycles:

CO_2 has excellent nuclear physical features, such as inertness at certain temperature range, stability, nontoxicity, a moderate value of critical temperature and pressure etc. Because of small size, high thermal efficiency, S- CO_2 has the potential to be more cost-effective and practical than typical working fluids cycles. In addition, it may lower the cost and duration of nuclear power station building by using modular construction technology. It has increasingly become a research hub and garnered a great deal of attention. Numerous configurations of the S-CO_2 Brayton power cycle have been suggested and examined for nuclear applications, and thermodynamic cycle calculation.

S-CO_2 gives better performance than steam and helium brayton cycle at considerably lower temperatures, making it particularly desirable at a variety of power temperatures and scales. As reported by Persichilli et al, the possible benefits of the S-CO_2 power cycle over Rankine cycle are improved thermal efficiency, high compactness, low turbomachinery cost etc. [6], [17], [18].

An outstanding distinguishing feature of S-CO_2 in contrast to constant property fluids is the severe fluctuation in all of the thermodynamic properties (density, specific heat, viscosity, thermal conductivity, and Prandtl number) at a certain temperature called pseudocritical temperature. The isobaric specific heat of a fluid reaches its maximum value at a given pressure at pseudocritical temperature, which resembles critical temperature. The physical properties of SCO_2 rapidly and nonlinearly vary close to the pseudocritical temperature. The characteristics of SCO_2 vary dramatically from fluids with constant properties because of this. The pseudocritical temperature rises together with the working pressure, and the change in the characteristics is less pronounced in the area further from the critical condition. Each attribute changes quickly and significantly as the working pressure gets closer to the critical pressure, which is close to the pseudocritical temperature. When heat energy is extracted from SCO_2 inside a gas cooler, the initial variance in the characteristics is modest and changes dramatically as the temperature approaches the pseudocritical point. As the working pressure reaches the critical pressure, the peak of the specific heat narrows and sharpens. S-CO_2 is superior to supercritical water as a heat transmission fluid in the gas cooler due to its lower critical parameters and reduced specific volume.[19]

There is a global drive to replace subcritical steam Rankine cycles with SCO_2 to reduce capital costs. Supercritical carbon dioxide shows some attractive thermodynamic properties near the critical condition. The critical state for carbon dioxide is 31.1 °C temperature and 7.38 MPa pressure. For these reasons, SCO_2 can be used as an alternative to steam plant. S-CO_2 has some advantages over the Rankine cycle listed below[20]:

- Supercritical CO_2 cycles have lower expansion ratio.
- Because of having very high temperature at turbine outlet, waste heat utilization is possible using recuperator.
- S-CO_2 cycles gives better performance than rankine cycles because of higher cycle maximum temperature.
- The fluid is compressed near the critical point. At this region, their density is higher. So, less work input is needed in compressor.
- Due to having supercritical state, the pinch point in heat exchangers is comparatively less.
- Total cost of the plant is comparatively lower.
- Since no phase change occurs, there is no necessity of bothering about dryness fraction.

1.5 Various proposed models of SCO_2 cycles:

Ma and Turchi designed multiple configurations for closed-loop sCO2 Brayton cycles in CSP facilities. High efficiency operation can be possible with turbine inlet temperatures between 500 and 700 degrees Celsius. Dostal et al. investigated a detailed analysis along with multiple-parameter optimization of the family of SCO2 Brayton cycles, demonstrating that the S-CO_2 cycle, in particular the recompression one, has comparable thermal efficiency to the helium Brayton cycle at significantly lower temperature [21–23]. Results reported that recompression S-CO_2 cycle has an efficiency of up to 47%. He investigated in details S-CO_2 Brayton cycles, revealing that at significantly lower temperature, S-CO_2 cycle, specifically the recompression one, has better thermal efficiency compared to the helium Brayton cycle. Besarati and Goswami compared various closed-loop supercritical cycles and found that the recompression and partial refrigeration cycle layout had efficiencies greater than fifty percent[24]. Kim et al improved the efficacy of the S-CO_2 recompression cycle based on the recuperator's efficiency and pressure point temperature restriction. [25] . Additionally, the division ratio and the pressure ratio were optimized. For the

analysis and optimization, Dyreby et al.[26] involved recuperation and recompression processes CO_2 Brayton cycles for reducing heat wastage. The thermodynamic state of the working fluid at main compressor inlet and ratio of operating pressures had a significant effect on the thermal efficiency. Padilla et al. reported a comprehensive exergetic analysis of different solar-assisted sCO2 closed-loop Brayton cycle configurations with recuperation and recompression. At 850 °C, they discovered that the recompression cycle offers the highest exergetic performance and thermal efficiency of 55.2%. The proposed sCO2 recompression cycle could be a viable option for central solar receiver systems[27, 28].

1.6 Applications of SCO_2 cycles:

Recent interest in concentrating solar power (CSP) has increased due to scope to recover CO_2 for the intermittent nature of other renewable energy sources. Al-Sulaiman and Atif analyzed the efficacy of various S-CO_2 cycle configurations integrated with a solar power structure. With a thermal efficiency of 52%, the recompression cycle model demonstrated impressive performance. At 50 °C compressor inlet temperature, S-CO_2 Brayton cycle attained a cycle efficiency of 43% if air cooling system is used for heat removal in heat exchanger.

Wang and He designed solar power tower linked with SCO_2 recompression cycle[29]. Reheating stages are included in this model. He utilized molten salt as medium for transferring heat. Zhang et al. explored the effects of thermal boundary conditions on the structure, layout and optimization of the heat source on the Rankine cycles overall performance using supercritical fluid. Milani et al. examined various SCO_2 cycle models connected with concentrated solar power systems He optimized the performance and input parameters. Song et al. conducted a thermal evaluation of the sCO2 cycles by improving the structure of preheater[30]. Padilla et al. through utilizing a dry refrigeration system, determined the thermal performance of different SCO_2 cycles configurations. Cycle having compression with intercooling at turbine inlet temperature of 850 degrees Celsius yielded the maximum cycle efficiency of 55.2%. Ishiyama et al. compared SCO2 cycle power generation systems with some other cycles like steam cycle, helium cycles etc [31]. They discovered that the SCO2 cycle bears desirable characteristics for the nuclear fusion reactor system prototype.

Chapter 2: Literature Review

2.1 Utilization of waste heat:

SCO_2 cycles have the benefits of a small footprint and high durability [32]. For applications on offshore platforms, selection of SCO_2 is highly suitable in electrical and mechanical purposes [33]. The S-CO_2 cycle pressure ratio is typically low. On the other hand, the maximum temperature of the cycle that lies at turbine inlet is very high. This substantial quantity of thermal burden should be utilized to enhance cycle efficiency. In S-CO_2 cycle systems, recuperators are commonly implemented. Here, because of suboptimal heat exchange efficiency the heat burden of the high temperature stream is not possible to be recovered entirely using regeneration technique. For this reason, a pre-cooler is required for discharging final low-grade heat to the atmosphere. If exhaust gas is directly discharged, significant quantities of thermal energy are lost[34]. Waste heat recovery (WHR) is an effective method for recovering unused heat and improving the thermal performance of a system [35]. Adding another cycle at bottom is a typical WHR technique. Because of having space constraints in platforms located at offshore, the bottoming cycle must adhere to certain constraints, like high thermal efficiency, improved power density, and reliability. The latest research indicates that the combined cycle system consisting of a gas-topping Brayton cycle and a steam-topping Rankine cycle is unsuitable gas turbine power stations of various sizes[36]. Marchionni et al. conducted a thermo-economic analysis of four distinct configurations of S-CO_2 bottoming cycle where he cascaded each configuration with a steam Rankine cycle in order to utilize residual heat[37]. Due to the fact that steam Rankine cycle requires a great deal of space and is not cost-effective for most largescale power facilities. Organic Rankine Cycle (ORC) is more appropriate for small-scale and low-grade heat sources due to its reduced thermal efficiency, lower power density, and working fluid limitations[38].

2.2 Organic Rankine Cycle as waste heat recovery:

ORC is a widely used alternative for recovering waste heat when the heat source temperature is below 370°C [39] .In prior studies, the combined cycle system consisting of an S-CO_2 cycle on top and an ORC on the bottom for gaining the wasted heat and run the ORC cycle was presented and analyzed[40–50]. Perez-Pichel et al. [51] merged an ORC with a S-CO_2 Brayton cycle configuration at the bottom for a sodium reactor and compared the performance enhancement with

other system optimizations including operating parameters adjustment and dual cycles having steam Rankine cycle integrated with. Several S-CO_2 cycle layouts having closed loops as well as combined cycle with ORC at the bottom were proposed by Chacartegui et al. [52] for solar power generation plants. These cycles represented optimistic innovations with the potential to compete with other conventional technologies in terms of efficacy and cost, according to preliminary results. Sanchez et al.[53] investigated a combined cycle consisting of S-CO_2 cycle and a trailing ORC. He used purified substances and also mélange of hydrocarbons. It is possible to achieve a 7% improvement in overall efficiency compared to standalone topmost S-CO_2 cycle. Simulation was conducted by Besarati integrating an ORC to different layouts of SCO_2 in solar field[54] .The results of simulation revealed that the recompression model of SCO_2 combined with ORC cycle obtained maximum thermal efficiency. Zhang et al. [55]performed analysis of performance of S-CO_2 cycle combined with an ORC in order to determine the influence of a number of crucial parameters on the performance of the system.

However, the efficacy of the cycle is significantly influenced by the choice of working fluid. Based on the slope of the saturation vapour curve in the T-s diagram, organic working fluids are typically divided into three categories.: moist (negative slope), isentropic (vertical slope), and dry (positive slope). Typically, the moist fluids must be superheated to prevent liquid particles from colliding with turbine blades at the time of expanding[56]. For ORC cycles, only dry fluids are used in this study. The working fluid attains saturated vapor state before entering the turbine. The environmental impact of using organic fluids must also be taken into account. Chacartegui et al. analyzed [57]the efficacy of a combined SCO_2–ORC cycle using various working fluids and operating conditions. Depending on the turbine inlet temperature, the results demonstrated that the efficacy of S-CO_2 was enhanced by 7–12% points. Notable is the fact that the uncomplicated S-CO_2 configuration was considered in this research. In a separate study, Sanchez et al. [58]analyzed the efficacy of a combined SCO_2–ORC cycle employing hydrocarbon compounds as ORC cycle working fluid. The results demonstrated that the composition of the mélange directly affects the efficacy of the cycle. At higher temperatures, supplementing the optimal pure fluid with a denser fluid improves efficiency, whereas at lower temperatures, doping with a lighter fluid result in better output.

2.3 Transcritical CO_2 cycle as waste heat recovery:

Apart from SCO_2 brayton cycles, the authors proposed a transcritical CO_2 cycle. This cycle has much different layout compared to SCO_2 cycle. For handling, high-density liquid and improve the system's performance, pump is used instead of compressor. Wright et al. conducted experiment on trans-critical CO2 cycle at the Sandia National Laboratory in which they observed an enhancement in cycle performance in comparison to the Rankine cycle. Between turbines, incorporating multiple reheat stage increased the efficiency by an additional 4–5%[59]. Wang et al.[60] performed research of a T-CO_2 power cycle's performance. The parameters were then optimized using a genetic algorithm in order to increase second law efficiency. Later on, they examined a solar-9 powered system that consists of cooling system integrated with heating system as well as power generation process[61]. This system uses T-CO_2 and an ejector-expansion mechanism. They discovered that rise in turbine back pressure of turbine and turbine intake temperature enhanced the system's efficiency. Song et al. presented a solar-powered T-CO_2 power cycle utilizing heat sink with cooling medium having LNG as working fluid[62]. They discovered that the overall power cycle efficiency may reach around 6.51 percent under certain conditions Yari and Sirousazar devised a T-CO_2 cycle for recovering waste heat from the precooler of a S-CO_2 Brayton cycle, and they estimated the performance enhancement of this novel combined cycle in comparison to a basic S-CO_2 cycle. Cao et al. also combined supercritical carbon dioxide cycle with trans-critical CO_2 cycle and he found 17% enhancement in performance compared to a ordinary regenerative cycle.[63]

According to the authors, their novel approach increased first and second law efficiencies by 5.5%, to 26%, and decreased exergy degradation by 6.7%, to 28.8%. Garg et al. compared trans-critical SCO2 cycle and steam Rankine cycle to determine volumetric flow rate and entropy production in CSP systems

2.4 Comparison between TCO_2 and ORC cycle:

The transcritical CO_2 power cycle (T-CO_2 cycle) can replace the organic rankine cycle (ORC) for recovering low-grade waste heat because it has better temperature glide between the working fluid

and heat source inside the vapour generator. Sarkar [64] reviews the T-CO_2 cycle literature, focusing on low-grade heat sources and working fluid performance. He concludes that T-CO_2 cycle has advantages over steam and organic Rankine cycles (ORC) and suggests ways to improve it (parameter optimization, hardware components, etc.). Wang and Dai examined the exergoeconomic performance of T-CO_2 and ORC bottoming cycles optimized for waste heat recovery from an S-CO_2 recompression Brayton topping cycle [65]. Parametric optimisation shows that the T-CO_2 bottoming cycle has better exergoeconomic performance than the ORC at lower pressure ratio (PRc) (off-design circumstances) and higher turbine inlet temperatures. ORCs had lower total product unit costs than other combined cycles. Chen et al. [66]tested two bottoming cycles that recover work from low-grade waste heat. The T-CO_2 power cycle outperformed the ORC. This cycle produced more power than ORC and had a pinch-limit-free heat exchanger. Most S-CO_2 power cycle studies used fixed heat exchanger effectiveness or pinch point temperature variations to describe heat exchanger performance, according to the literature. Chen et al. later compared the T-CO_2 cycle to an ORC using R123 in ORC cycle. T-CO_2 at bottom produced more energy than ORC integrated. Cayer et al.[67]analyzed two CO_2 transcritical power cycle topologies. They also investigated performance using six different metrics[68]. Chen et al. [69] performed a comparative study between TCO_2 and ORC for utilizing unused heat. In ORC, he used R123 as the working fluid. Finally, it was found that TCO_2 cycle generates more work as output in comparison to ORC operating at same condition.

2.5 Research scopes:

Several studies on the S-CO_2 cycle and the T-CO_2 cycle were conducted further. In recent age, research has also been conducted on the performance of the combined S-CO_2 T-CO_2 cycles. But research for both configurations (combined SCO_2 ORC and SCO_2 TCO_2) uses simple and recompression cycle as topping cycle and partial cooling cycle in rare case. In this study, we have focused on partial cooling and another model of SCO_2 cycle which is main compression SCO_2 along with recompression cycle. Moreover, research works till now integrated only one bottoming cycle with a topping cycle. For partial cooling and main compression layout, two bottoming cycles can be integrated with each cycle as two precoolers. In this study, two different bottoming cycles, one is TCO_2 and the other is ORC is integrated to each of the SCO_2 cycles. Parameter optimisation

was carried out with regard to various critical parameters in order to investigate the behaviour of combined cycles. Additionally, integrated cycle models are compared to one another. The analysis showed that the maximum temperature of the S-CO_2 cycle improved the thermal efficiency of the combined cycle. Due to pseudocritical effects, MCIT improves performance up to 40-45° C before declining. The energy efficiency of the combined cycle rises initially when the turbine intake pressure in the TCO_2 cycle is raised, but this benefit is temporary. However, condensation temperature at the bottom of the cycle reduces effectiveness. S-CO_2 cycle with bottoming cycle merged showed considerably enhanced performance compared to standalone cycle values. In addition, it is discovered that the primary compression with intercooling models provide the best performance

Chapter 3: Description of the model/System

In this research, 3 different model of S-CO_2 cycles are taken into consideration. In each of the model, bottoming cycle is integrated with the topping S-CO_2 cycle. Throughout this study, two different categories of cycles have been emphasized as bottoming cycles, one is T-CO_2 cycle and the other is ORC. In the first model, recompression S-CO_2 cycle is merged with T- CO_2 cycle. Second model includes a partial cooling S-CO_2 merged with one is transcritical CO_2 cycle and one ORC. The third model main compression S-CO_2 cycle combined with T-CO_2 and ORC. Now let us see in details about each of the proposed models, their configurations and working principle

3.1 Combined Recompression S-CO_2 T-CO_2 cycle (RC + TCO_2):

This model represents a combined cycle consisting of recompression S-CO_2 cycle and T-CO_2 cycle. The configuration of this model is shown in figure 1. The recompression cycle model is a kind of similar to the simple brayton cycle with some additional components like recompressor, HTR and LTR. In the topping cycle, required input heat energy is applied to the cycle at the heater (point 4 to 5). At the outlet of the heater (point 6), the working fluid reaches its maximum temperature which is the turbine inlet temperature (TIT). Work is obtained as output at the turbine with the expansion of the working fluid (point 5 to 6) to the minimum operating pressure of the cycle. From the turbine outlet, the low-pressure fluid is passed through the HTR (point 6 to 7) which is followed by LTR (point 7 to 8). Inside HTR, the low-pressure stream rejects heat at constant pressure. This rejected heat is gained by another stream entering the HTR (point 3 to 4). Coming out of the HTR, the low-pressure stream passes through the LTR. As like HTR, the working fluid undergoes isobaric heat rejection. Next, the working fluid is splitted into two streams (point 8). One stream passes through the heat recovery, precooler and main compressor and the other stream enters the recompressor. Inside heat recovery (point 8 to 9), the working fluid rejects heat. This heat is utilized by the bottoming transcritical CO_2 cycle. The working fluid stream of the topping cycle is further cooled to the main compressor inlet condition using precooler (points 9 to 1). Inside the main compressor, work is supplied as input to the system and compression occurs to the maximum pressure of the cycle (state 2). The process is adiabatic process. Then, this stream enters into the LTR (point 2 to 3) where it absorbs heat from the low -pressure stream (point 7 to 8). The other stream passes through the recompressor where additional work is supplied as

input to the cycle. At the LTR outlet (point 8), both the splitted streams merge together. This combined stream now enters the high temperature recuperator (HTR). Inside HTR, gaining the heat rejected from the low- pressure stream (point 6 to 7), the stream reaches the state 4. Now, heat is again applied as input to the working fluid through the reactor. This same cycle is repeated again and again.

In bottoming cycle, the working fluid lies below the critical point at saturated liquid state at the pump inlet. Using pump, T-CO_2 fluid is pressurized to turbine inlet pressure of the bottoming cycle from point 1t to 2t. The upper pressure of the TCO_2 cycle is set above the critical point of carbon dioxide. So, the working fluid converts from subcritical to supercritical state. In this cycle, heat energy gained from the topping cycle is utilized, no additional heat source is used. As heat is added at constant pressure, the temperature rises form point 2t to point 3t. After that, the working fluid goes through the turbine where work is generated as output. From the turbine we get the output work. It is to be mentioned that using turbine. the T-CO_2 fluid is expanded to the pump inlet pressure, which lies below the critical pressure. For this reason, during expansion inside turbine, the fluid transforms from its supercritical to subcritical state. Then the working fluid is now cooled using condenser to its saturated liquid state (point 1t). Fig 2 represents the T -S diagram of the working principle of the whole combined cycle

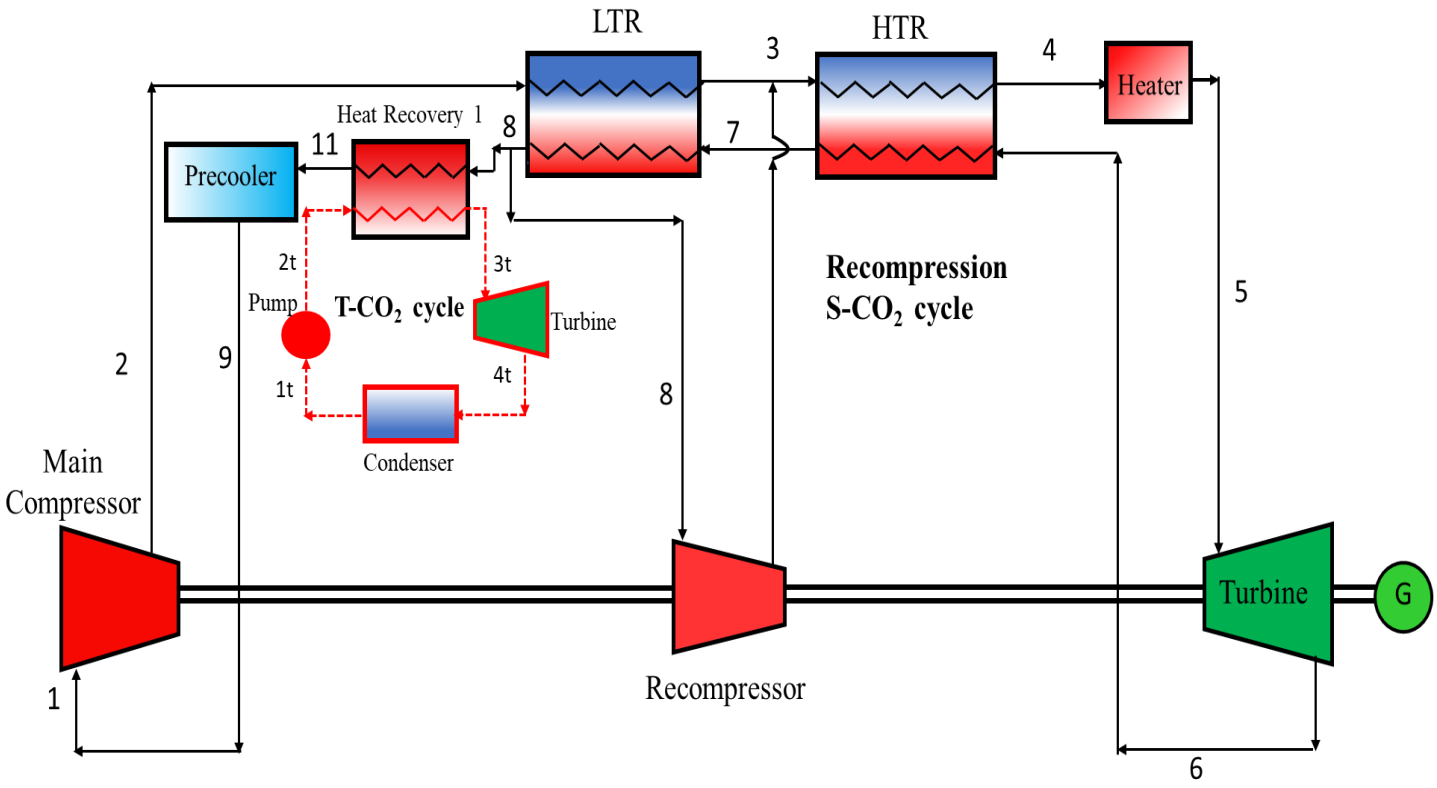

Fig 1: Schematic diagram of Combined Recompression S-CO_2 T-CO_2 cycle

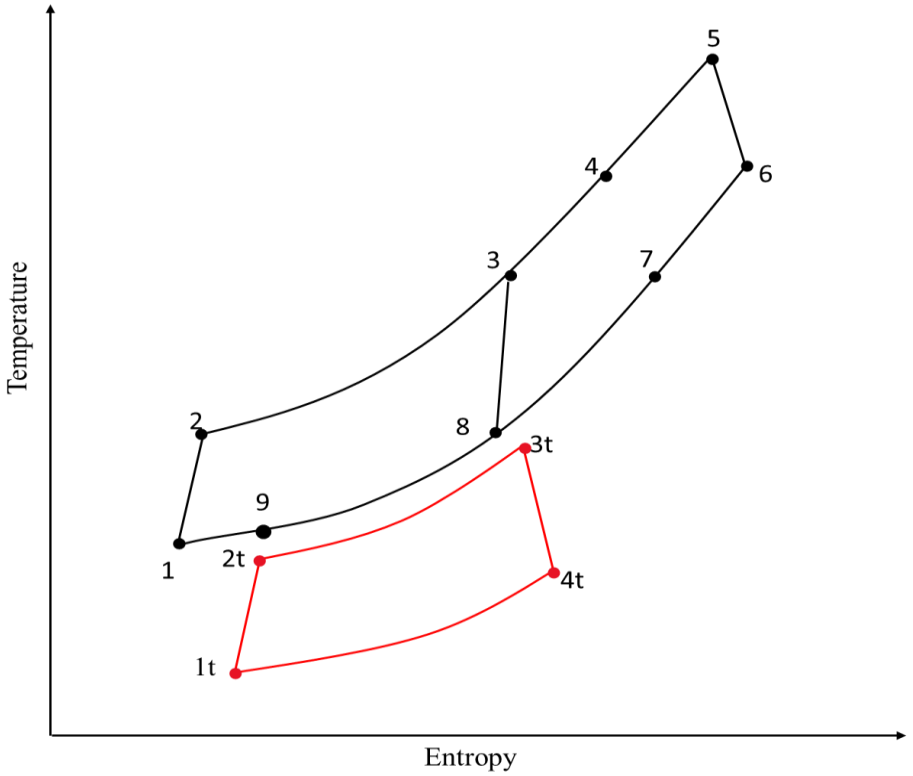

Fig 2: T-S diagram of Combined Recompression S-CO_2 T-CO_2 cycle

3.2 Combined Partial Cooling S-CO_2 T-CO_2 ORC cycle (PC + TCO_2+ORC):

This model represents a partial cooling S-CO_2 cycle which is merged with a transcritical CO_2 and an ORC. The structure of this whole model is shown in fig 3. The additional component used in the topping cycle is the precompressor. In this model, after expansion at the turbine outlet, low pressure stream of the working fluid is passed through the HTR and LTR. Here, heat energy is released from the low-pressure stream. After coming out of the LTR, the SCO_2 fluid is passed through the heat recovery 1. In this heat recovery, T-CO_2 cycle is integrated with the topping cycle. Releasing heat, the working fluid reaches from point 8 to 11. Using precooler, the working fluid is reached to the point 9. In this study, the temperature at point 9 is considered equal to that of point 1 which is the main compressor inlet temperature. Next, the working fluid is compressed from minimum pressure to intermediate pressure of the cycle using precompressor. Just at the outlet of the precompressor, the stream is splitted into two sections. One flows through the recompressor and the other passes through the main compressor and other components. Using recompressor, the working fluid is further compressed to its maximum pressure from intermediate

pressure. The other stream first passes through heat recovery 2 where ORC cycle is integrated with the upper cycle (point 10 to 12). Now, using precooler, compressor inlet state is reached. At the main compressor, the required work input is supplied. Working fluid is pressurized from its intermediate pressure to maximum pressure. After that, this high-pressure stream enters the LTR where it receives the heat energy rejected by the hot stream. At the outlet of the LTR, two fluid streams again merges with each other. Now, this combined stream passes through the HTR. As like LTR, the heat lost by the low- pressure stream is absorbed by this stream. Required heat energy is supplied at the heater.

The T-CO_2 cycle layout and working principle is similar to that of the recompression cycle. The layout is simple rankine cycle consisting of pump, turbine, condenser. Instead of heater, heat recovery is used. In this cycle, the upper pressure lies beyond the critical point of CO_2. But the lower pressure lies just a little below the critical pressure. At the outlet of the pump, the fluid remains at its saturated liquid state. Using pump, the fluid is pumped from its saturated state to supercritical state beyond its critical point (point 1t to 3t). This working fluid is now heated using the rejected heat from the heat recovery 1. Thus, it reaches at point 3t. Now the fluid is expanded at the turbine where energy is extracted as work output (point 3t to 4t). Coming out of the turbine, the fluid passes through the condenser where it is condensed back to point 1t (saturated liquid state)

In the ORC cycle, dry refrigerants (having positive slope of vapour saturation curve) are used as working fluid. The layout of this cycle is also like simple Rankine cycle. Here cycle absorbs heat from the topping cycle, gets converted in to vapour. At the outlet of the heat recovery, the refrigerant is maintained at saturated vapour state (point 3o). The fluid undergoes expansion through the turbine. Here, condensation pressure is achieved. Next heat is rejected in the condenser. After rejecting heat, the organic fluid reaches the saturated liquid state at the condensation temperature (point 1o). Next, fluid is pressurized in the pump from its lower pressure to higher pressure.

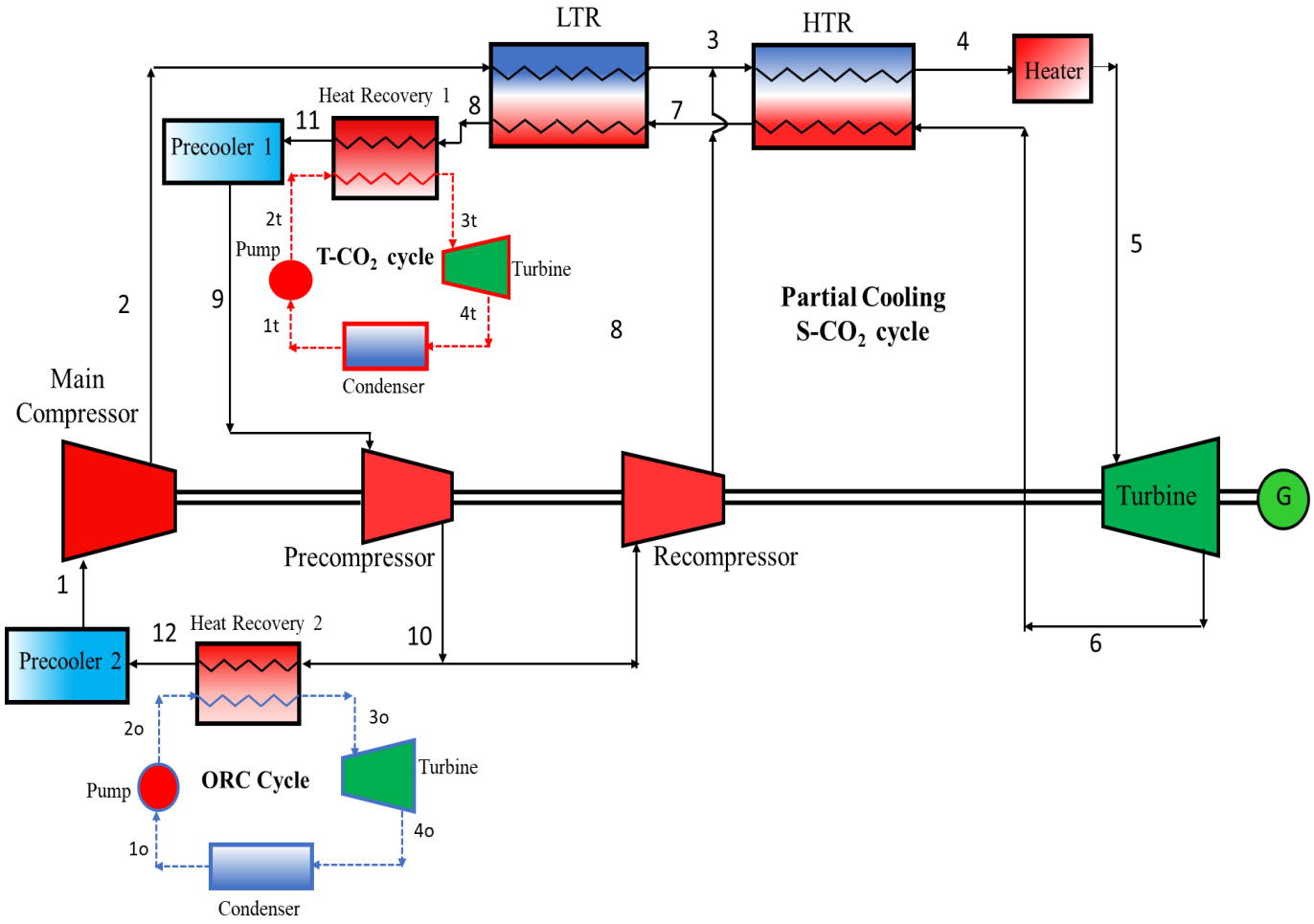

Fig 3: Schematic diagram of Combined Partial cooling S-CO_2 T-CO_2 ORC cycle

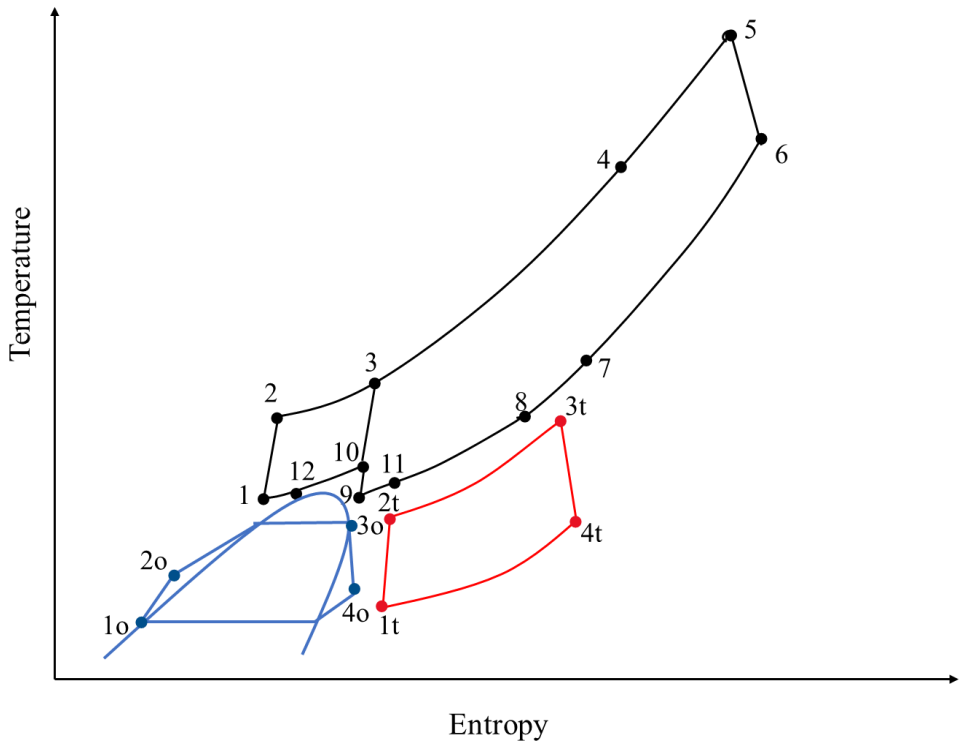

Fig 4: T-S diagram of Combined Partial Cooling S-CO_2 T-CO_2 ORC cycle

3.3 Combined Main Compression S-CO_2 T-CO_2 ORC cycle (MC + TCO_2+ORC):

This model represents combined cycle where main compression S-CO_2 cycle merged with T-CO_2 and ORC. This model is almost similar to partial cooling model. The only difference is the location of the recompressor in the topping cycle. Here the recompressor is connected at the LTR outlet (point 8).

As like the aforementioned models, a low-pressure stream of the working fluid is transmitted through the LTR and HTR after expansion at the turbine outlet. The low -pressure stream releases thermal energy at these two components. Exiting from the LTR (point 8), the working fluid is divided into two sections, one stream is compressed from lower to higher pressure using recompressor. Another stream successively flows through the two heat recoveries, precompressor and two precoolers. In thermal recovery 1, the T-CO_2 cycle and the topping cycle are combined. The working fluid reaches from point 8 to 11 by releasing heat. Through the use of a precooler,

the operating fluid is cooled to point 9. Similar to the combined partial cooling cycle, the temperature at point 9 is kept equal to the cycle lowest temperature. Using precompressor, the working fluid is then compressed from minimum pressure to intermediate pressure of the cycle. Next, this stream traverses heat recovery 2, where the ORC cycle is incorporated with the upper cycle (points 10 to 12). Using a precooler, the compressor inlet state has been attained. At the primary compressor, the necessary work input is provided. The working fluid's intermediate pressure is increased to its utmost pressure. This high-pressure stream then enters the LTR, where it receives the rejected thermal energy from the hot stream. At the outflow of the LTR, two fluid streams once again converge. Currently, this combined stream traverses the HTR. As with LTR, this stream absorbs the heat lost by the low-pressure stream. The heater is furnished with the necessary heat energy.

The architecture and operating principle of the T-CO_2 cycle are exactly similar to those of the recompression cycle. The design is a straightforward rankine cycle consisting of a compressor, turbine, and condenser. In lieu of a heater, heat recovery is utilized. In this cycle, the upper pressure exceeds the CO_2 critical pressure. The lower pressure, however, rests just below the critical pressure. At the pump's discharge, the fluid maintains its saturated liquid state. The fluid is propelled from its saturated state to its supercritical state beyond its critical point (point 1t to point 3t) using a pump. This working fluid is now heated with heat rejected from heat recovery 1. Therefore, it reaches point 3t. Now the fluid is expanded at the turbine, which extracts energy as work output (points 3t to 4t). The fluid exiting the turbine passes through the condenser, where it is condensed back to point 1t (state of saturated liquid) releasing heat to the external environment.

In the ORC cycle, as the working fluid in the ORC cycle, dry refrigerants with a positive slope of the vapour saturation curve are utilized. The structure of this cycle resembles that of the simple Rankine cycle. This cycle absorbs the heat from the topping cycle and transforms it into vapour. At the heat recovery's outlet, the refrigerant is maintained in a saturated vapour state (point 3o). The fluid expands as it passes through the turbine. At this point, condensation pressure is reached. Next, the condenser rejects the heat. The organic fluid reaches the saturated liquid state at the condensation temperature (point 1o) after rejecting heat. Next, the pump increases the pressure of

the fluid from its lower pressure to its higher pressure. The layout and TS diagram of the whole cycle combination is shown in the figure 5 and 6

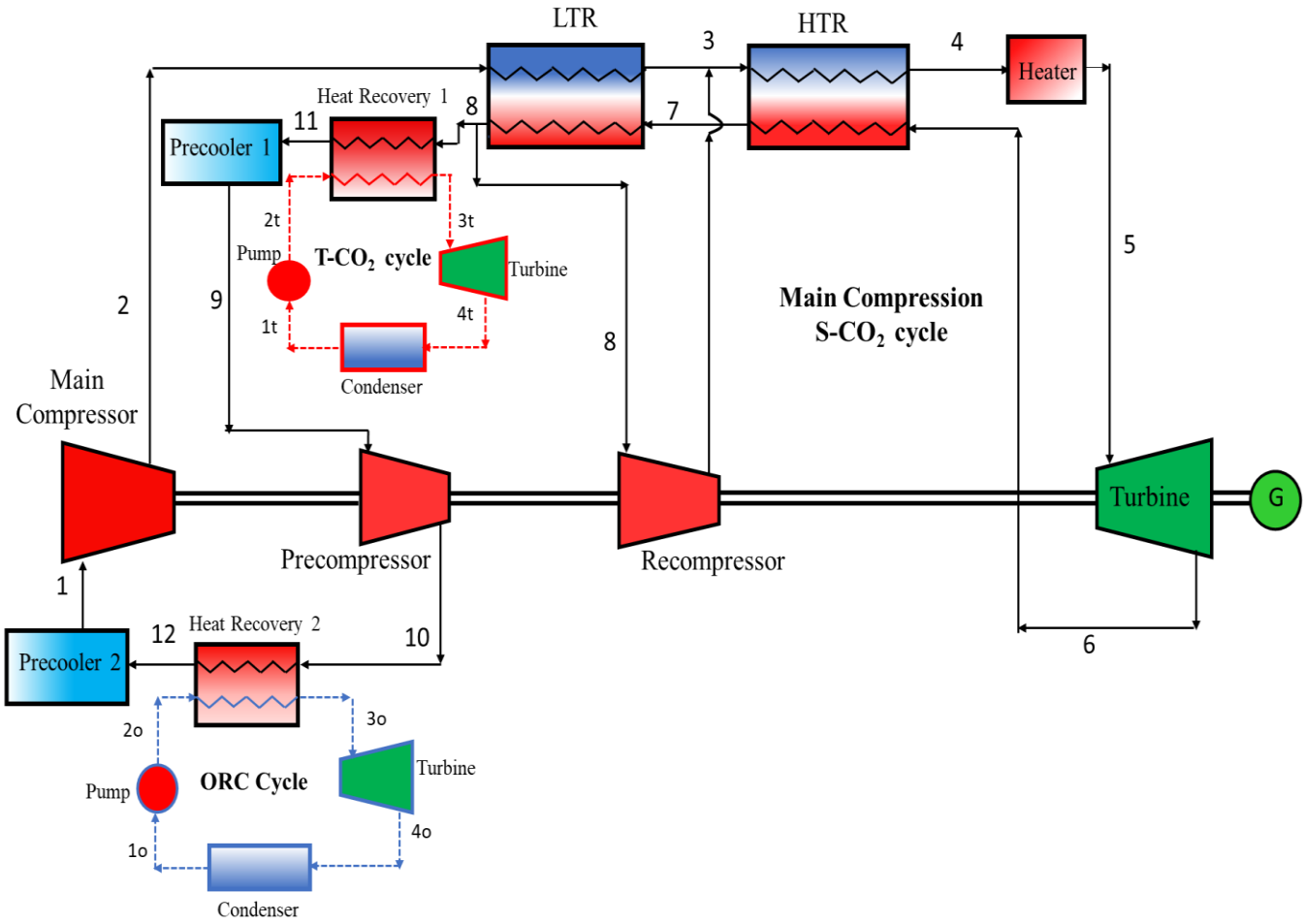

Fig 5: Schematic diagram of Combined Main Compression S-CO_2 T-CO_2 ORC cycle

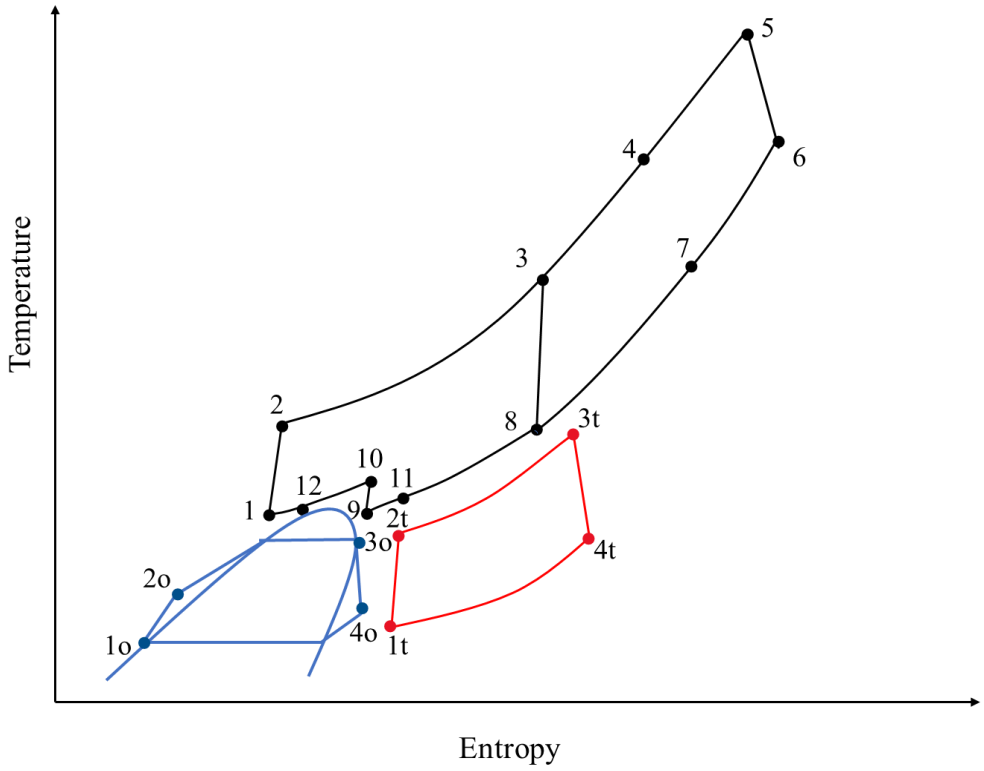

Fig 6: T-S diagram of Combined Main Compression S-CO_2 T-CO_2 ORC cycle

3.4 <u>Performance Comparison between different possible combinations</u>:

In this study, we have been using TCO_2 and ORC as bottoming cycles. For the combined Partial cooling SCO_2 TCO_2 ORC model and Main compression SCO_2 TCO_2 ORC model, two bottoming cycles are integrated. Here, instead of using the combinations of figure 3 and 5, some other combinations are also possible using the two same bottoming cycles. Possible combinations other than the mentioned one are discussed below:

- <u>S-CO_2 + T-CO_2 + T- CO_2</u>: Without using any organic rankine cycle, both the bottoming cycles used the transcritical cycles.
- <u>S-CO_2 + ORC +ORC</u>: In this model, 2 ORC cycles having same layout, refrigerants are integrated with a single partial cooling and main compression cycle.
- <u>S-CO_2 + ORC +T-CO_2</u>: This configuration has same as that of the one shown in figure 3 and figure 5. The exceptional part is that the position of ORC and transcritical CO_2 is

altered. Here the ORC is merged with the topping cycle at the heat exchanger 1 and T-CO_2 cycle is merged at heat recovery 2

Each of the proposed models are applicable for both partial cooling and main compression cycle. In figure 7, performance comparison between these possible models is shown where the topping cycle is partial cooling cycle. In figure 7a, comparison is done in terms of thermal efficiency whereas exergy efficiency comparison is shown in figure 7b. Both these comparison reveals that the configuration having T-CO_2 cycle connected with heat recovery 1 and ORC cycle at heat recovery 2 gives best performance. The configuration having 2 ORC cycles gives best performance second to the aforementioned model. The combination with 2 T-CO_2 cycles give lowest performance

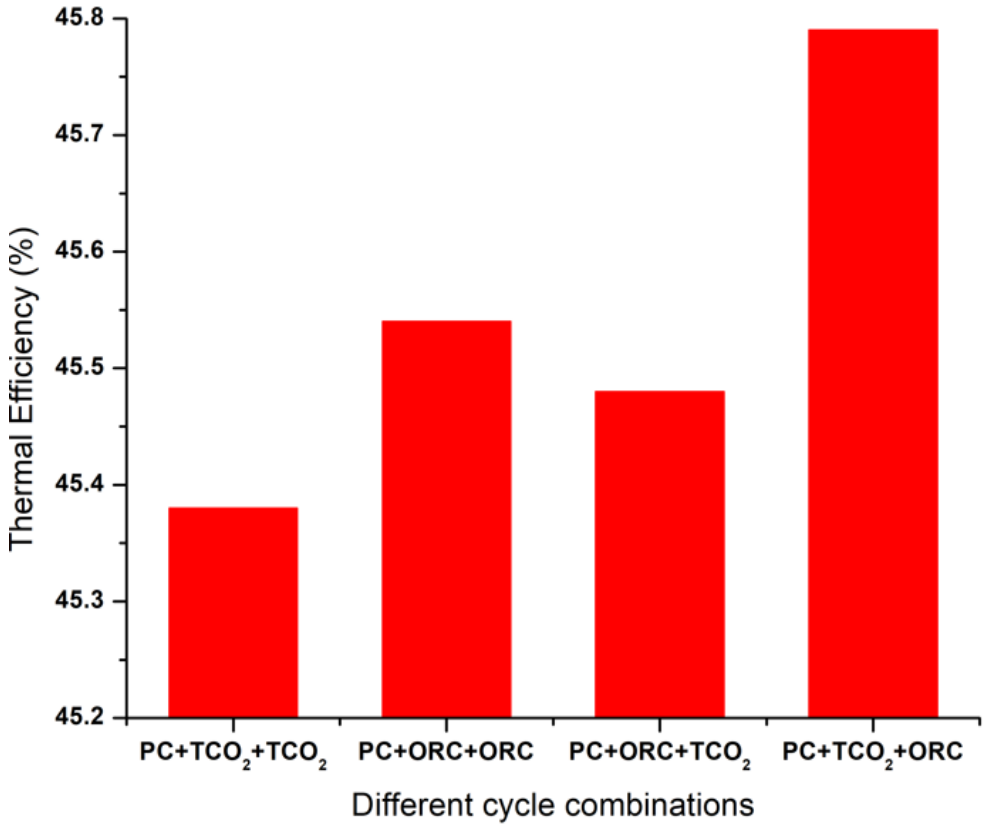

(a) Thermal Efficiency comparison

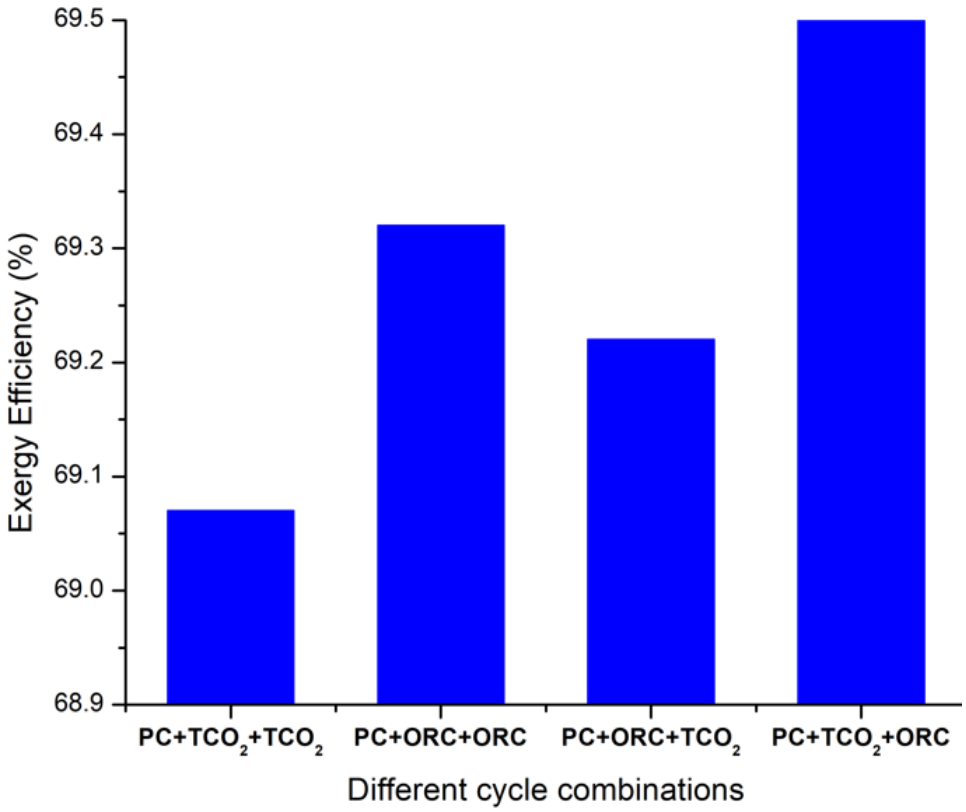

b) Exergy Efficiency comparison

Figure 7: Performance comparison between possible layouts of Partial Cooling S-CO_2 cycle

Figure 8 represents performance comparison between the alternative models when main compression model of SCO_2 is used as the topping cycle. From the comparison, we can see that the combined cycle configuration having T-CO_2 cycle at heat exchanger 1 and ORC at heat exchanger 2 gives comparatively better result than other combinations. Here, the combination having the position of T-CO_2 and ORC altered shows lowest efficiency in terms of both thermal and exergy efficiency. Figure 8a compares the combinations in terms of thermal efficiency, while figure 8b compares the combinations in terms of energy efficiency. From each of these graphs, it is clear that the model which we have used so far (PC + TCO_2+ORC) and (MC + TCO_2+ORC) is much superior to the other combinations in terms of both thermal and exergy efficiency. For this reason, this model has been focused throughout this study

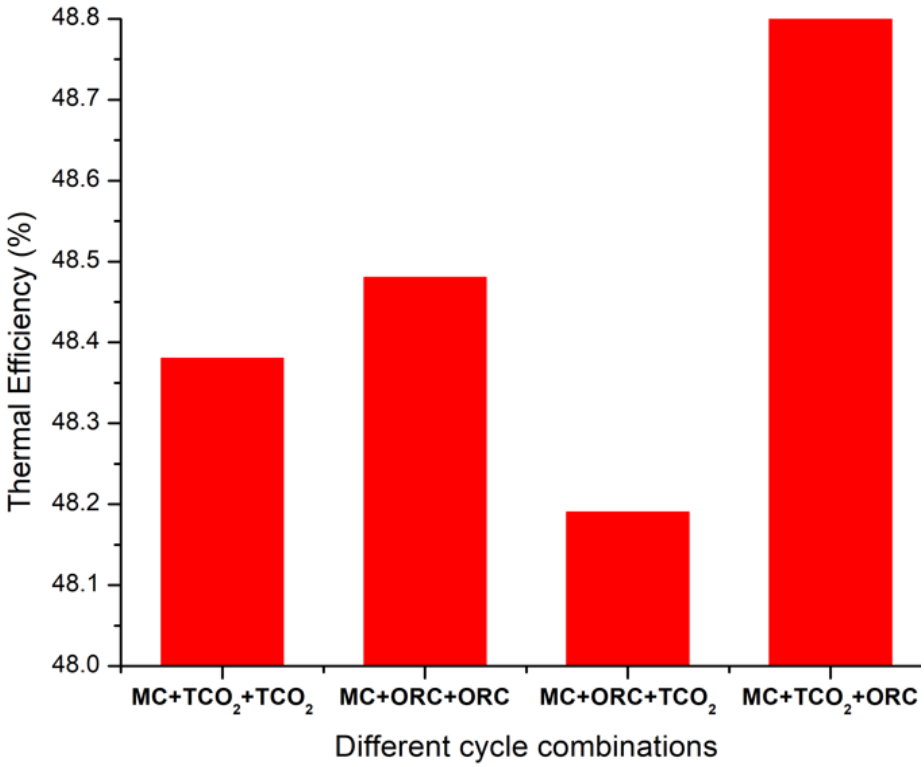

(a) Thermal Efficiency comparison

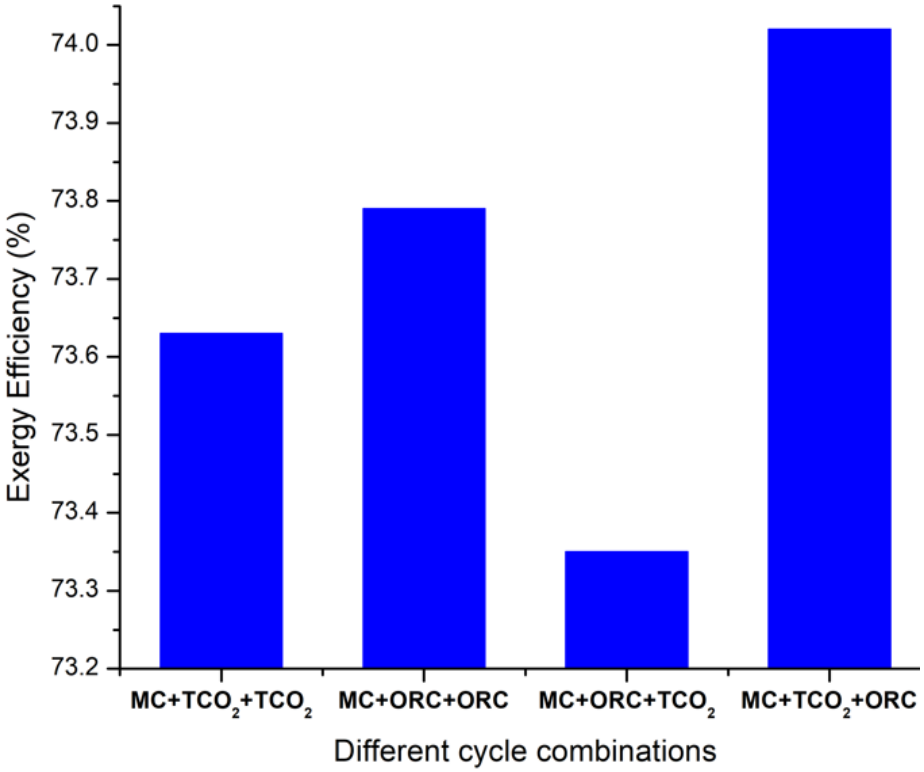

(b) Exergy Efficiency comparison

Figure 8: Performance comparison between possible layouts of Combined Main Compression cycle

Chapter 4: Methodology

4.1 Stated assumptions:

For conducting parametric analysis and comparison between performance of 3 different configurations, assumption of some basic parameters is to be done. Table 1 represents the values of the assumptions considered for parametric analysis in this study along with the boundary conditions at which the cycles are operated. The values are taken from relevant journals. The thermodynamic properties are taken from latest version of Coolprop library.

Table 1: Assumptions considered for parametric analysis of the combined cycle configurations

Parameters	Values
S-CO_2 turbine isentropic efficiency	93%
T-CO_2 turbine isentropic efficiency	85%
ORC turbine isentropic efficiency	85%
Main Compressor isentropic efficiency	89%
Pump isentropic efficiency	85%
Heat recovery effectiveness	95%
Main compressor inlet temperature(K)	308.15
Turbine inlet temperature of S-CO_2 (K)	1073.15
Maximum pressure of S-CO_2 cycle (MPa)	25
Minimum Pressure of S-CO_2 cycle (MPa)	7.5
Intermediate Pressure of S-CO_2 cycle (MPa)	10
Pinch Temperature (K)	5
Turbine Inlet Pressure of T-CO_2 cycle (MPa)	10
Condensation Temperature of T-CO_2 cycle	293.15
Condensation Temperature of ORC cycle	293.15
Ambient Temperature (K)	288.15
Temperature at heat source (K)	1080
Mass flow rate of S-CO_2 cycle (kg/s)	1
Refrigerant of ORC	R245fa

4.2 Energy Equations:

In each of the different combined cycle layouts, the output work is obtained from the turbine. Turbine extracts hydraulic energy from the fluid and convert it into mechanical work. Here, for each of the model, the equations are presented in the tables below:

Table 2: Energy equations for each of the components of the SCO_2 cycle

Components	Recompression SCO_2 cycle	Partial Cooling SCO_2 cycle	Main Compression SCO_2 cycle
Turbine	$W_1 = \dot{m}_S(h_5 - h_6)$	$W_1 = \dot{m}_S(h_5 - h_6)$	$W_1 = \dot{m}_S(h_5 - h_6)$
Main compressor	$W_2 = \dot{m}_S x(h_2 - h_1)$	$W_2 = \dot{m}_S x(h_2 - h_1)$	$W_2 = \dot{m}_S x(h_2 - h_1)$
Recompressor	$W_3 = \dot{m}_S(1 - x)$ $(h_3 - h_8)$	$W_3 = \dot{m}_S(1 - x)$ $(h_3 - h_{10})$	$W_3 = \dot{m}_S(1 - x)$ $(h_3 - h_8)$
Precompressor	------	$W_4 = \dot{m}_S(h_{10} - h_9)$	$W_4 = \dot{m}_S x(h_{10} - h_9)$
Heater	$Q_{in} = \dot{m}_S(h_5 - h_4)$	$Q_{in} = \dot{m}_S(h_5 - h_4)$	$Q_{in} = \dot{m}_S(h_5 - h_4)$
HTR	$(h_6 - h_7) = (h_4 - h_3)$	$(h_6 - h_7) = (h_4 - h_3)$	$(h_6 - h_7) = (h_4 - h_3)$
LTR	$(h_7 - h_8) = x(h_3 - h_2)$	$(h_7 - h_8) = x(h_3 - h_2)$	$(h_7 - h_8) = x(h_3 - h_2)$
Heat Recovery 1	$\dot{m}_S x(h_8 - h_{11})$ $= \dot{m}_t(h_{3t} - h_{2t})$	$\dot{m}_S(h_8 - h_{11})$ $= \dot{m}_t(h_{3t} - h_{2t})$	$\dot{m}_S x(h_8 - h_{11})$ $= \dot{m}_t(h_{3t} - h_{2t})$
Precooler 1	$Q_{loss} = \dot{m}_S x(h_9 - h_1)$	$Q_{loss} = \dot{m}_S(h_{11} - h_9)$	$Q_{loss} = \dot{m}_S x(h_{11} - h_9)$
Heat Recovery 2	-------	$\dot{m}_S x(h_{10} - h_{12})$ $= \dot{m}_t(h_{3o} - h_{2o})$	$\dot{m}_S x(h_{10} - h_{12})$ $= \dot{m}_t(h_{3o} - h_{2o})$
Precooler 2	$Q_{loss} = \dot{m}_S x(h_9 - h_1)$	$Q_{loss} = \dot{m}_S(h_{12} - h_1)$	$Q_{loss} = \dot{m}_S x(h_{12} - h_9)$

Table 3: Energy equations for each of the components of the T-CO_2 cycle

Components	Equations
Turbine	$W_5 = \dot{m}_t(h_{3t} - h_{4t})$
Pump	$W_6 = \dot{m}_t(h_{2t} - h_{1t})$
Condenser	$Q_{loss} = \dot{m}_t(h_{4t} - h_{1t})$

Table 4: Energy equations for each of the components of the ORC cycle

Components	Equations
Turbine	$W_7 = \dot{m}_t(h_{3o} - h_{4o})$
Pump	$W_8 = \dot{m}_o(h_{2o} - h_{1o})$
Condenser	$Q_{loss} = \dot{m}_o(h_{4o} - h_{1o})$

The net work done by the combined cycle is equal to the resultant of the work done by the each of the components of the cycle. Resultant work done can be calculated as follows

$$W_{net} = W_1 - W_2 - W_3 - W_4 + W_5 - W_6 + W_7 - W_8$$

Overall thermal efficiency

$$\eta = \frac{W_{net}}{Q_{in}}$$

4.3 Exergy Analysis :

Now , let us describe the equations related to exergy change at each of the components of the cycle. At a certain point in the cycle , exergy can be calculated by the following equation

$$X = m[(h_i - h_0) - T_o(s_i - s_o)]$$

At the heater , Exergy input occurs with the addition of heat the cycle . The amount of exergy input

$$X_{in} = (1 - \frac{T_0}{T_r})Q_{in}$$

At each and every component, there is always loss in exergy. Exergy loss at each component

$$X_{loss} = \Sigma X_{in} - \Sigma X_{out} + \Sigma W_{in} - \Sigma W_{out}$$

Table 5: Exergy equations for each of the components of S-CO_2 cycle

Components	*Recompression cycle*	*Partial Cooling cycle*	*Main compression cycle*
Turbine	$X_{dest,t} = \dot{m}_s[(h_5 - h_6) - T_o(s_5 - s_6)] - W_{out}$	$X_{dest,t} = \dot{m}_s[(h_5 - h_6) - T_o(s_5 - s_6)] - W_{out}$	$X_{dest,t} = \dot{m}_s[(h_5 - h_6) - T_o(s_5 - s_6)] - W_1$
Main compressor	$X_{dest,c} = \dot{m}_s x[(h_1 - h_2) - T_o(s_1 - s_2)] + W_{in}$	$X_{dest,c} = \dot{m}_s x[(h_1 - h_2) - T_o(s_1 - s_2)] + W_{in}$	$X_{dest,c} = \dot{m}_s x[(h_1 - h_2) - T_o(s_1 - s_2)] + W_2$
Recompressor	$X_{dest,r} = \dot{m}_s x[(h_8 - h_3) - T_o(s_8 - s_3)] + W_{in}$	$X_{dest,r} = \dot{m}_s x[(h_{10} - h_3) - T_o(s_{10} - s_3)] + W_{in}$	$X_{dest,r} = \dot{m}_s x[(h_8 - h_3) - T_o(s_8 - s_3)] + W_3$

Precompressor	------	$X_{dest,p} = \dot{m}_s[(h_9 - h_{10}) - T_o(s_9 - s_{10})] + W_{in}$	$X_{dest,p} = \dot{m}_s x[(h_9 - h_{10}) - T_o(s_9 - s_{10})] + W_4$
Heater	$X_{in} = (1 - \frac{T_0}{T_r})Q_{in}$	$X_{in} = (1 - \frac{T_0}{T_r})Q_{in}$	$X_{in} = (1 - \frac{T_0}{T_r})Q_{in}$
HTR	$X_{dest,HTR} = \dot{m}_s[(h_3 - h_4) - T_o(s_3 - s_4)] + \dot{m}_s[(h_6 - h_7) - T_o(s_6 - s_7)]$	$X_{dest,HTR} = \dot{m}_s[(h_3 - h_4) - T_o(s_3 - s_4)] + \dot{m}_s[(h_6 - h_7) - T_o(s_6 - s_7)]$	$X_{dest,HTR} = \dot{m}_s[(h_3 - h_4) - T_o(s_3 - s_4)] + \dot{m}_s[(h_6 - h_7) - T_o(s_6 - s_7)]$
LTR	$X_{dest,LTR} = \dot{m}_s x[(h_2 - h_3) - T_o(s_2 - s_3)] + \dot{m}_s[(h_7 - h_8) - T_o(s_7 - s_8)]$	$X_{dest,LTR} = \dot{m}_s x[(h_2 - h_3) - T_o(s_2 - s_3)] + \dot{m}_s[(h_7 - h_8) - T_o(s_7 - s_8)]$	$X_{dest,LTR} = \dot{m}_s x[(h_2 - h_3) - T_o(s_2 - s_3)] + \dot{m}_s[(h_7 - h_8) - T_o(s_7 - s_8)]$
Heat Recovery 1	$X_{dest,recov\,1} = \dot{m}_s x[(h_8 - h_{11}) - T_o(s_8 - s_{11})] + \dot{m}_t[(h_{2t} - h_{3t}) - T_o(s_{2t} - s_{3t})]$	$X_{dest,recov\,1} = \dot{m}_s[(h_8 - h_{11}) - T_o(s_8 - s_{11})] + \dot{m}_t[(h_{2t} - h_{3t}) - T_o(s_{2t} - s_{3t})]$	$X_{dest,recov\,1} = \dot{m}_s x[(h_8 - h_{11}) - T_o(s_8 - s_{11})] + \dot{m}_t[(h_{2t} - h_{3t}) - T_o(s_{2t} - s_{3t})]$
Precooler1	$X_{dest,precooler\,1} = \dot{m}_s x[(h_{11} - h_9) - T_o(s_{11} - s_9)]$	$X_{dest,precooler\,1} = \dot{m}_s[(h_{11} - h_9) - T_o(s_{11} - s_9)]$	$X_{dest,precooler\,1} = \dot{m}_s x[(h_{11} - h_9) - T_o(s_{11} - s_9)]$
Heat Recovery 2	------	$X_{dest,recov\,2} = \dot{m}_s x[(h_{10} - h_{12}) - T_o(s_{10} - s_{12})] + \dot{m}_t[(h_{2o} - h_{3o}) - T_o(s_{2o} - s_{3o})]$	$X_{dest,recov\,2} = \dot{m}_s x[(h_{10} - h_{12}) - T_o(s_{10} - s_{12})] + \dot{m}_t[(h_{2o} - h_{3o}) - T_o(s_{2o} - s_{3o})]$

Precooler 2	------	$X_{dest,precooler\ 2} = \dot{m}_s x[(h_{12} - h_1) - T_o(s_{12} - s_1)]$	$X_{dest,precooler\ 2} = \dot{m}_s x[(h_{12} - h_1) - T_o(s_{12} - s_1)]$

Table 6: Exergy equations for each of the components of the T-CO_2 cycle

Components	Equations
Turbine	$X_{dest,t} = \dot{m}_t[(h_{3t} - h_{4t}) - T_o(s_{3t} - s_{4t})] - W_5$
Pump	$X_{dest,pump} = \dot{m}_t[(h_{1t} - h_{2t}) - T_o(s_{1t} - s_{2t})] + W_6$
Condenser	$X_{dest,cond} = \dot{m}_t[(h_{4t} - h_{1t}) - T_o(s_{4t} - s_{1t})]$

Table 7: Exergy equations for each of the components of the ORC cycle

Components	Equations
Turbine	$X_{dest,t} = \dot{m}_o[(h_{3o} - h_{4o}) - T_o(s_{3o} - s_{4o})] - W_7$
Pump	$X_{dest,pump} = \dot{m}_o[(h_{1o} - h_{2o}) - T_o(s_{1o} - s_{2o})] + W_8$
Condenser	$X_{dest,cond} = \dot{m}_o[(h_{4o} - h_{1o}) - T_o(s_{4o} - s_{1o})]$

Exergy Efficiency of the combined cycle

$$\eta_{ex} = \frac{W_{net}}{X_{in}}$$

4.4 Model Validations:

Prior to the thermodynamic study of combined SCO_2 ORC cycles, validation of different standalone SCO_2 configurations was done. The reference was taken from the research work on advanced supercritical carbon dioxide cycle by Turchi, Wagner, Neises and Zhiwan[70] . Figure 9 and 10 denotes the comparison between the reference data and the data obtained thermodynamic analysis. Here in each of the cases, single stage reheat turbine is used. Figure 9 shows the variation of cycle performance due to change in turbine inlet temperature. Each of the cycle configurations shows better performance with the rise in cycle maximum temperature. Figure 10 represents comparison between the calculated efficiency and the reference value of the efficiency when the minimum temperature of the cycle is varied keeping the other parameters unchanged. In this case, lower cycle minimum temperature gives better performance. Both these figures show that the reference value graph and the graph are almost overlapping. There is very small deviation of not more than 1% at some locations. So, it can be assured that the validation is appropriate

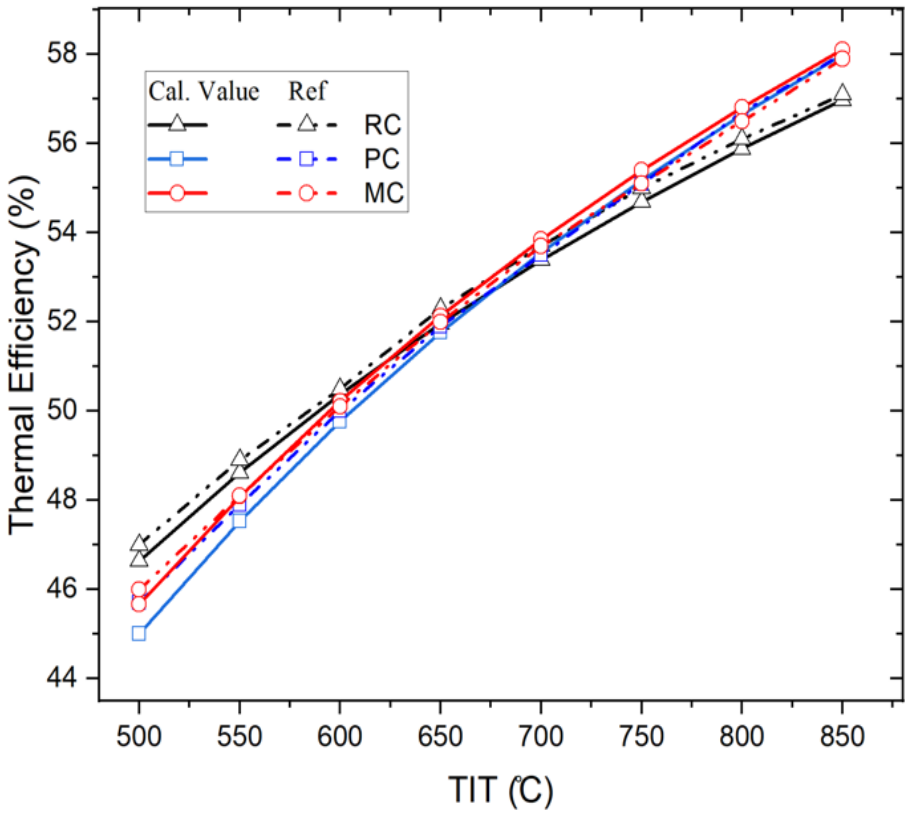

Figure 9: Validation using cycle maximum temperature

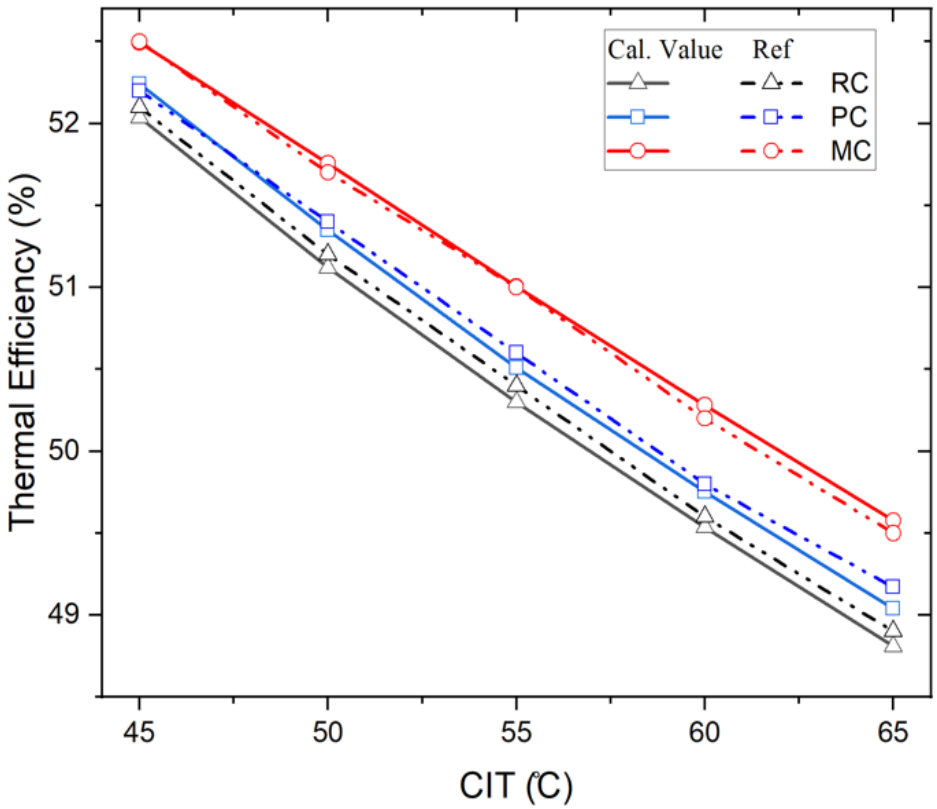

Figure 10: Validation using cycle minimum temperature

4.5 Framework of mathematical model:

In this research work, we have been dealing with 3 different combined cycle configurations. Considering the steps required to model the cycles in programming language, a flowchart is designed. Flowchart is made mainly focusing on the Combined Main compression S-CO_2 T-CO_2 ORC. It is represented in fig 4.

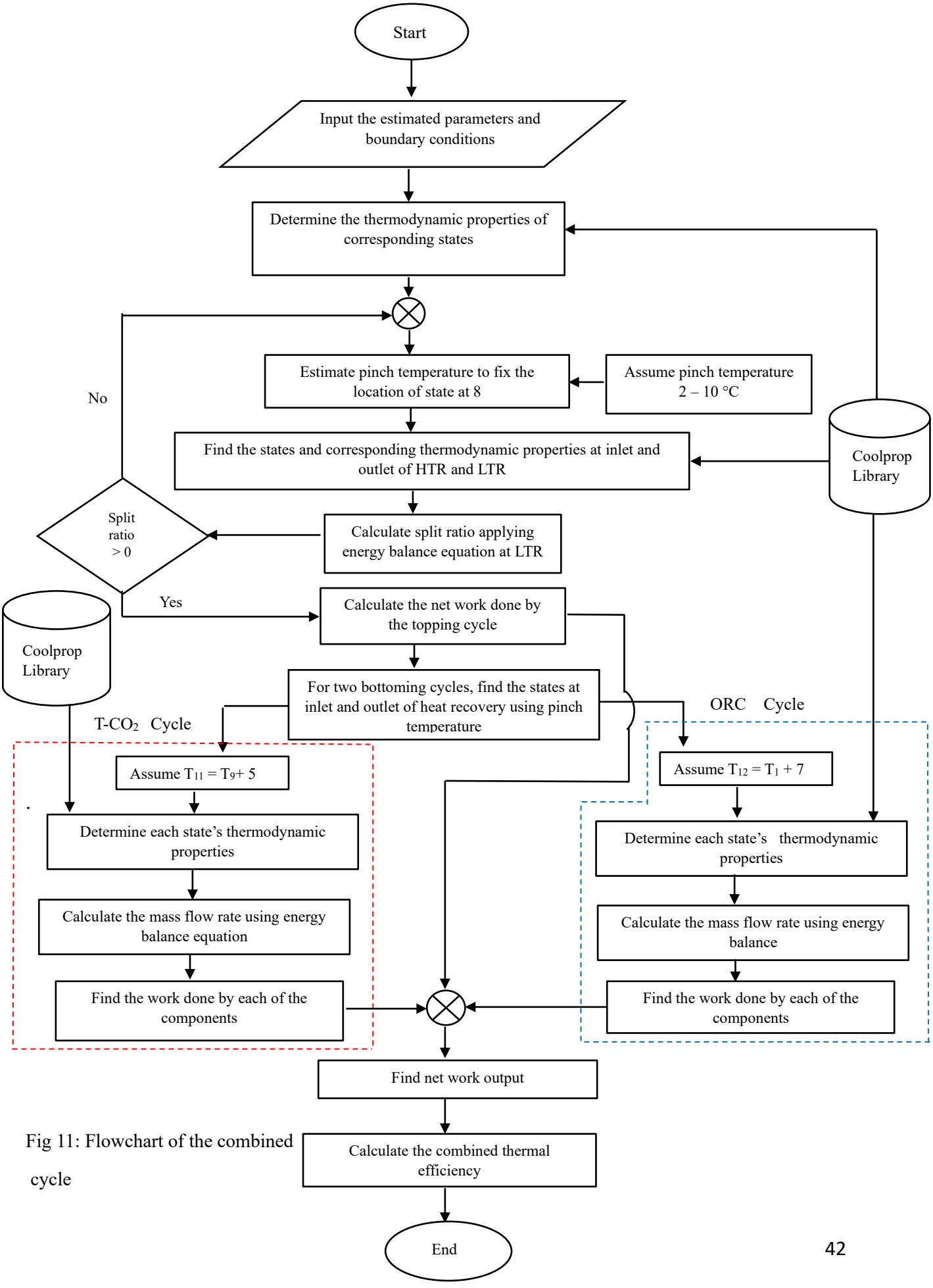

Fig 11: Flowchart of the combined cycle

Chapter 5: Results and Discussions

In this section, the results of the thermodynamic analysis of the each of the combined S-CO_2 T-CO_2 ORC cycles are presented. In table 1, values of certain operating parameters and boundary conditions have been assumed at which the cycles can be operated properly. At these assumed conditions, detailed performance of the combined cycles in shown in table 2 along with work obtained as output and work required as input for each of the components.

Table 8: Performance of the 3 different combined SCO_2 TCO_2 ORC cycles

Parameters	Recompression SCO_2 TCO_2	Partial Cooling SCO_2 TCO_2 ORC	Main Compression SCO_2 TCO_2 ORC
Thermal efficiency (%)	56.734	52.99	56.3
Exergy Efficiency (%)	77.38	72.27	76.8
Net power Output (kw)	155.8	179.258	169.8
Heat input (kw)	274.607	338.308	301.534
SCO_2 turbine work (kw)	196.51	206.411	206.411
Main compressor work (kw)	26.644	18.116	16.025
Recompressor work (kw)	20.03	7.157	20.173
Precompressor work (kw)	-----	9.321	6.747
TCO_2 turbine work (kw)	8.327	4.483	3.450
TCO_2 pump work (kw)	2.365	1.902	1.457
ORC turbine work (kw)	-----	4.918	4.351
ORC pump work (kw)	-----	0.058	0.052

From table 8, it is seen that the efficiency of partial cooling cycle SCO_2 TCO_2 ORC is comparatively lower than other models, whereas the thermal efficiency of the combined recompression and combined main compression SCO_2 TCO_2 ORC are almost same, a little bit difference can be seen. But the power output of combined partial cooling cycle is comparatively higher. In terms of heat energy input to the cycle, combined partial cooling cycle requires 338.3 kw whereas combined recompression and main compression cycle needs 274.6 and 301.534kw energy for operating at the stated conditions. Thus, it can be observed that the partial cooling cycle model comparatively takes more input energy also gives more work as output in comparison to the other proposed cycle models, still its efficiency is comparatively lower. Among the work producing and work consuming components, it is clear that major portion of the work is derived from the topping S-CO_2 cycle. Some additional work is added by the bottoming cycles.

Table 9: Exergy destruction at each of the components of the combined cycle

Components	Recompression SCO_2 TCO_2 (kw)	Partial Cooling SCO_2 TCO_2 ORC (kw)	Main Compression SCO_2 TCO_2 ORC (kw)
Exergy input	201.3405	248.045	221.083
Main compressor	2.316	1.734	1.534
LTR	4.087	2.67	4.153
HTR	12.899	33.112	18.306
Heater	8.898	14.048	10.964
SCO_2 Turbine	6.962	7.385	7.385
Precompressor	----	0.9	0.652
Recompressor	1.317	0.578	1.436
Cooler 1	2.706	1.558	1.128
TCO_2 pump	6.303	0.274	0.204
Heat Recovery 1	2.294	0.793	0.631
TCO_2 turbine	1.316	0.777	0.596
TCO_2 condenser	2.313	0.785	0.605
Cooler 2	----	2.242	1.983
ORC pump	----	0.00867	0.00767
Heat Recoverey 2	----	0.132	0.11675
ORC turbine	----	0.709	6.272
ORC condenser	----	1.076	0.95249

Table 9 represents the exergy loss at each of the components of the cycle when operated at boundary conditions of table 1. Exergy loss is mostly significant at the components of the topping cycle. At the bottoming cycles, exergy loss is very less. In all the models, the maximum exergy loss occurs at the High Temperature Recuperator. In combined SCO_2-TCO_2-ORC cycles, exergy input to the cycle is maximum, which is 248.045 kw. In recompression and Main compression cycle, it is 201.34 and 221.083 kw. For the combined recompression model, the lowest exergy loss occurs a the TCO_2 turbine. The minimum exergy destruction occurs at the ORC pump for partial cooling and main compression SCO_2-TCO_2-ORC cycle.

To achieve the best performance, it is currently necessary to obtain the effects of key parameters on the SCO_2-TCO_2-ORC power cycles. The main parameters that we have emphasized are Turbine Inlet Temperature, Main compressor Inlet temperature, recuperator effectiveness, TCO_2 turbine inlet pressure, condensation temperature of TCO_2, pressure ratio of both the bottoming cycles and different kinds of refrigerants. Table 2 shows the performance of each of the components of 3 different proposed models. These results are determined at the boundary conditions mentioned in table 1. Now let us see the results of the parametric analysis performed with respect to these specific parameters.

5.1 Impact of Turbine Inlet Temperature (TIT):

Turbine inlet temperature is the maximum temperature of the combined cycle which lies at the outlet of the heater (point 5). In figure12, analysis is done taking the maximum temperature of the topping cycle. Figure 12a shows the thermal efficiency variation and figure 12b shows exergy efficiency variation. These graphs also include comparison between the proposed combined cycle and the corresponding standalone S-CO_2 cycle. Results reveal that the thermal efficiency of both standalone cycle and topping cycle increases with the increase in turbine inlet temperature. For a particular pressure ratio, at higher temperature, the difference in enthalpy is more for isentropic condition. More enthalpy difference causes greater work generation at the turbine finally resulting in improved thermal efficiency. Thus, higher the temperature at the turbine inlet, more is the efficiency. For analysis, the range of cycle maximum temperature is considered about 550-900°C. For each of the models, combined cycle gives about 2-2.5% better performance than the standalone

cycle. In terms of exergy, the combined cycle models obtain 3.5 – 4% efficiency. Compared to the other models, the main compression model gives better performance for temperature upto 750°C. Beyond this temperature, recompression cycle generates better performance. Similar kind of impact can be observed in case of exergy. Better efficiency can be obtained through increasing the maximum temperature of the cycle. Though higher temperature gives improved performance, considering metallurgical limit of the components, fuel economy, heater effectiveness and all other related factors, the temperature at heater outlet is chosen to be 800 °C.

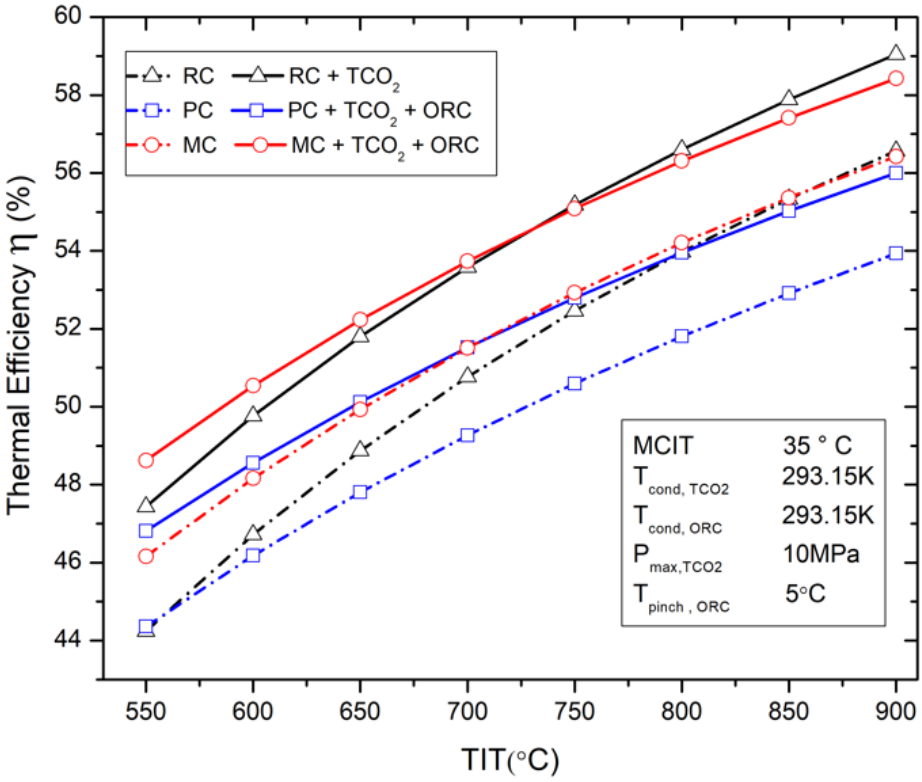

(a) Energy efficiency vs TIT

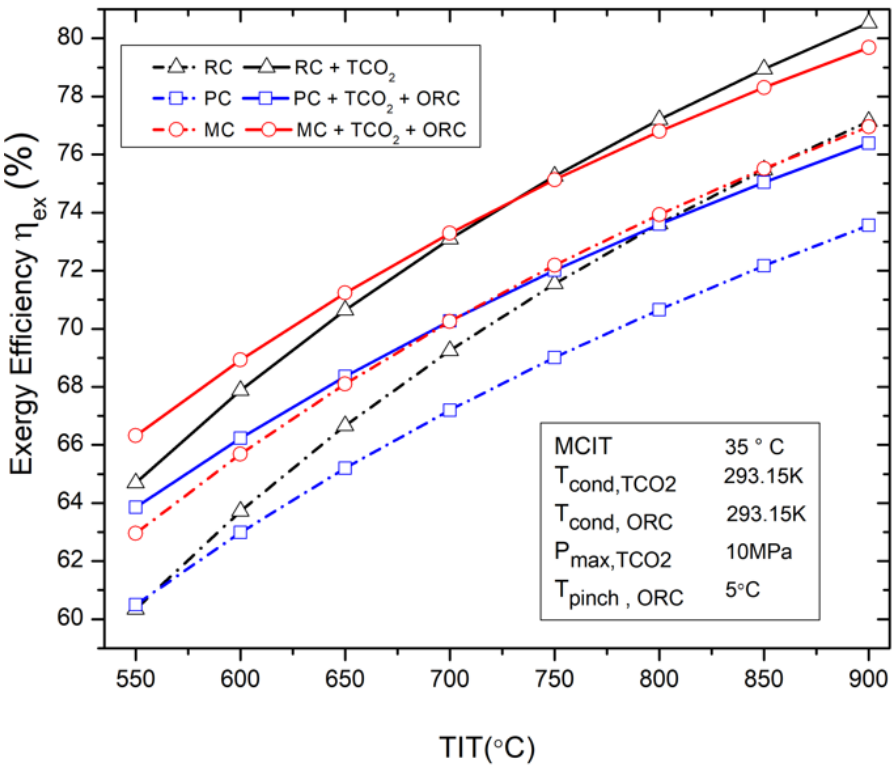

(b) Exergy efficiency vs TIT

Fig 12: Analysis of combined SCO_2 TCO_2 ORC configurations using cycle maximum temperature

5.2 Impact of Main Compressor Inlet Temperature (MCIT):

The lowest temperature of the topping cycle lies at the inlet of the main compressor. This temperature has significant effect on the performance of the whole cycle. Figure13 shows that increase in main compressor inlet temperature causes reduction in the thermal and exergy efficiency of the cycle. For standalone cycle, efficiency reduces with the increase in MCIT. Only exception can be seen in case of partial cooling cycle. For combined cycles, thermal efficiency increases upto 40 – 45° C for combined partial cooling and main compression cycle. Then efficiency starts to decline. The combined recompression cycle shows almost linear reduction in efficiency with the rise in MCIT similar to the standalone cycle. Lower temperature at compressor inlet causes enthalpy change to decrease at constant pressure ratio. For this reason, because of increase in MCIT, the work input required for the cycle also increases which causes decrease in overall efficiency of the cycle. The critical temperature of CO_2 is 31.1°C and critical pressure is

7.38MPa. At MCIT near the critical temperature, pseudocritical effects are significant. At temperature upto 40 - 45° C, exceptional variations in thermodynamic properties are present. For this reason, the performance rises at the initially. The temperature at the compressor inlet is kept within above 32°C due to critical point, proper functioning of the bottoming cycles. From fig 13(a), it can be seen that combined cycles give 2-3.5% more thermal efficiency. With the increase of MCIT, the difference in standalone and combined cycle model becomes more significant. For exergy, fig 13(b) depicts that 3- 4.5% better efficiency can be achieved in combined cycles.

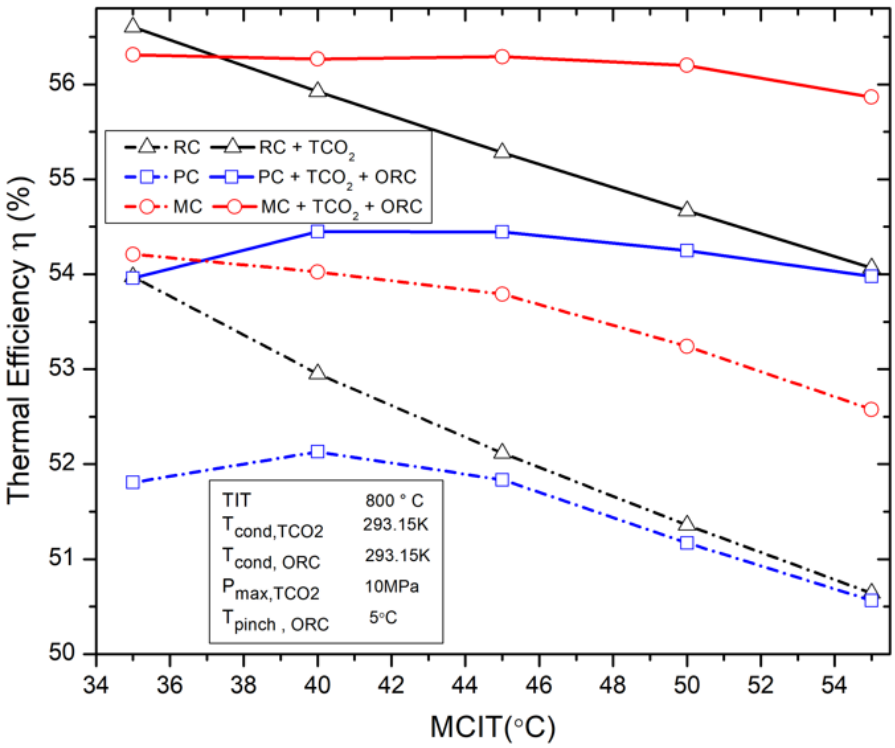

(a) Energy efficiency vs MCIT

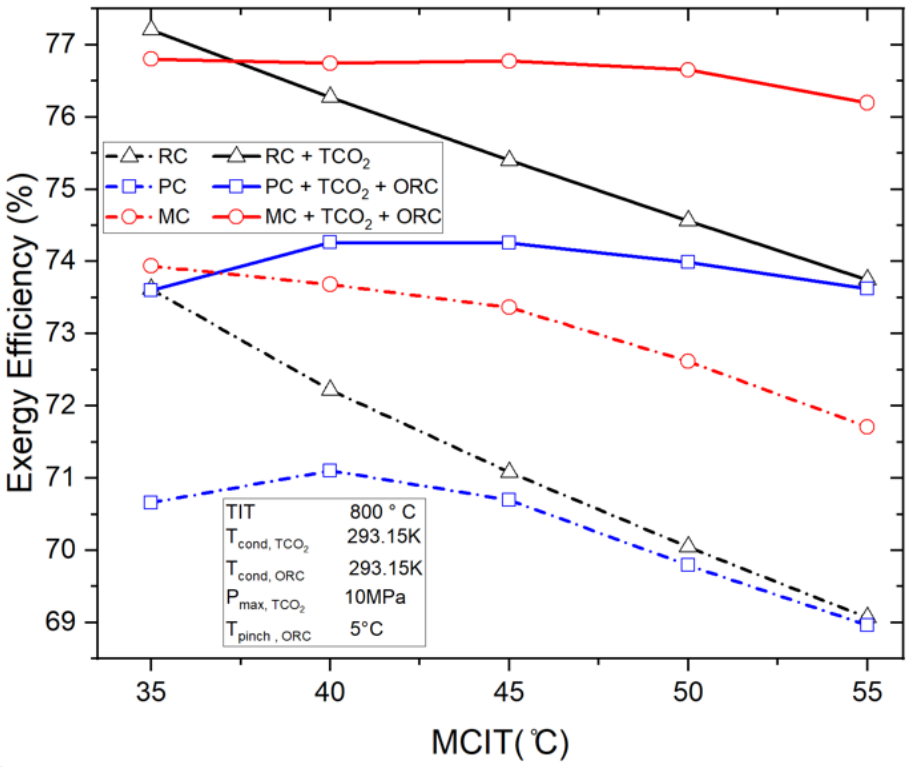

b) Exergy efficiency vs MCIT

Fig 13: Analysis of combined SCO_2 TCO_2 ORC configurations using main compressor inlet temperature

5.3 Impact of Recupearator Effectiveness:

Two recuperators are used in order the utilize the waste energy as much as possible. Variation in the effectiveness of recuperator causes slight change in the efficiency of the cycle. For analysis, the effectiveness in recuperator is considered from 0.9 limited to 0.98. With the increase in recuperator effectiveness, better use of waste energy occurs which results in better performance. The graphs (Fig 14) shows that thermal and exergy efficiency increases slightly with the increase in effectiveness. High effectiveness of recuperator requires complex design, high thermal conductivity, large size, high maintenance etc. Fig 14a depicts that for recompression and main compression cycle, combined model gives 2-2.5% better thermal efficiency compared to standalone cycle. Partial cooling cycle also gives about 2% better performance than standalone case though its efficiency is comparatively less than the other two models.

.

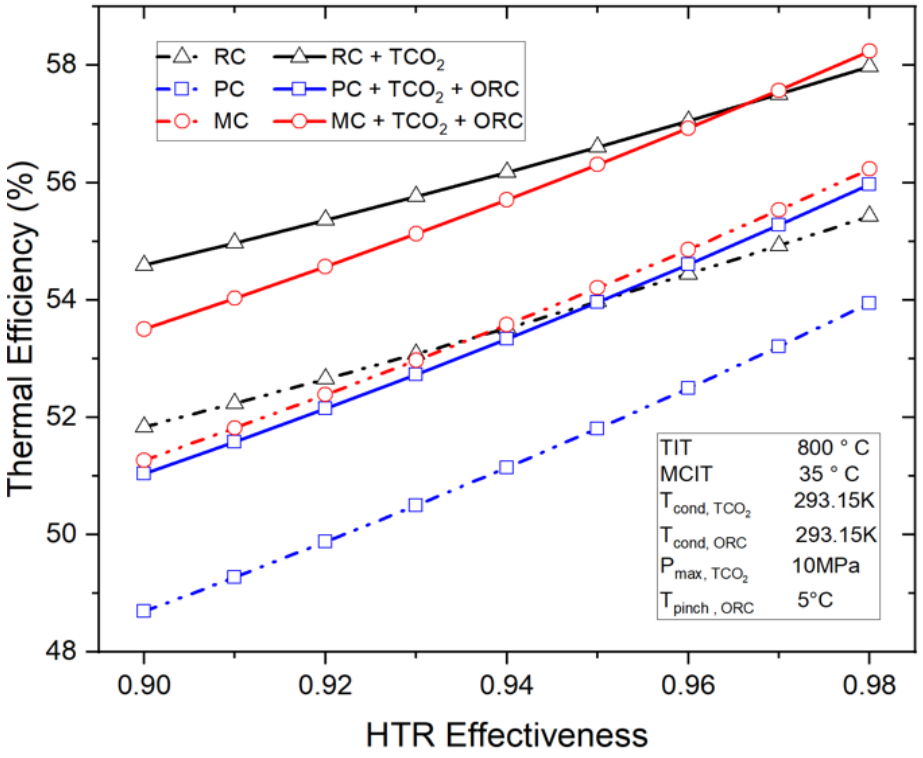

a) Energy efficiency vs recuperator effectiveness

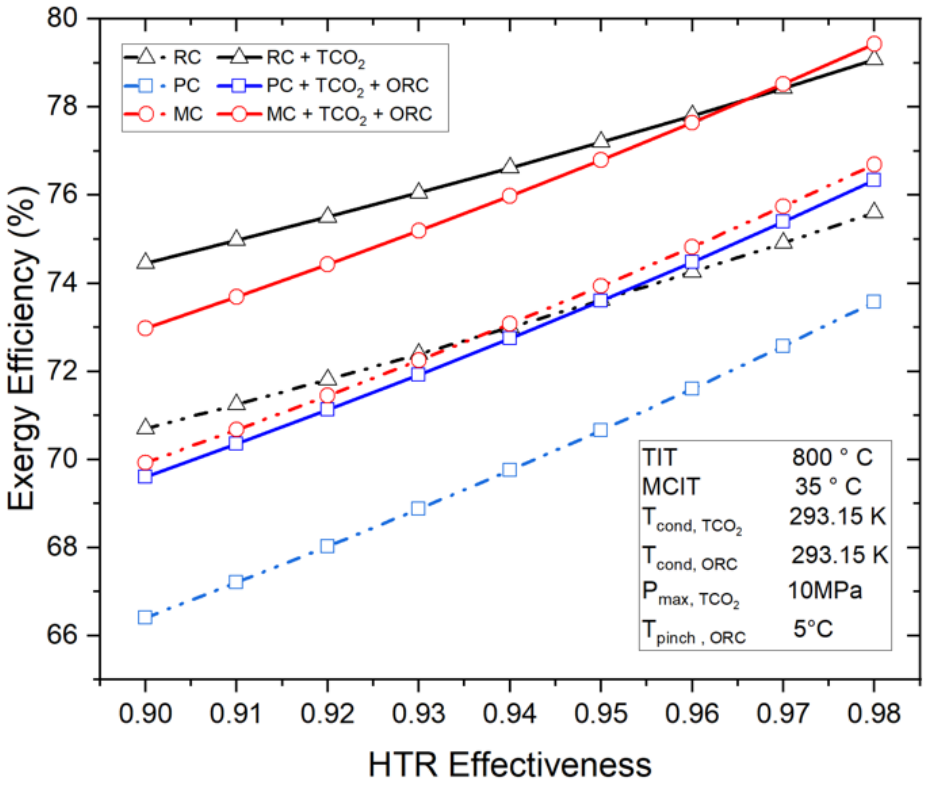

(b) Exergy efficiency vs recuperator effectiveness

Fig 14: Analysis of combined SCO_2 TCO_2 ORC configurations using HTR effectiveness

Figure 14b shows the variation of performance in terms of exergy. The variations look similar to that thermal efficiency. Each of the combined cycle models give approximately 3% more exergy efficiency than standalone model. Among the combined cycles, partial cooling cycle model gives less efficiency in comparison to other models. At effectiveness 0.9 to 0.96, recompression cycle has more efficiency than main compression model. Beyond effectiveness 0.96, main compression cycle model gives a little bit more efficiency than recompression cycle model in terms of both thermal and exergy. It is to be mentioned that for this parametric analysis, only the effectiveness of HTR is taken into consideration. For LTR, pinch point is used for determining the boundary conditions.

5.4 Impact of Turbine Inlet Pressure of TCO_2 cycle:

Turbine Inlet Pressure is the upper pressure of the TCO_2 cycle. At this pressure, the working fluid always lies at the supercritical state. So, this must be always higher than the critical pressure of carbon dioxide (7.38MPa). Parametric analysis is conducted taking turbine inlet pressure (TIP) of the bottoming T-CO_2 cycle. Since TIP is a parameter of TCO_2 cycle, it has no relation with the performance of standalone cycle. For partial cooling and main compression cycle, Fig 15a shows that the thermal efficiency increases with increase in TIP upto a certain value beyond which the efficiency starts declining. According to the graphs, the maximum thermal efficiency can be achieved pressure 11.5 to 12 MPa. For recompression cycle, performance continues to rise upto 15 MPa. Beyond that, there is gradual decrease in performance. Combined partial cooling cycle obtains net output power about 15kw more than combined main compression cycle model in every cases. Recompression cycle gives lesser output power than main compression model by 10-20 kw. Similar is the case for exergy analysis. From Fig 15b, we can observe that the exergy destruction occurs minimum when TIP lies within 10-11 MPa for combined partial and main compression cycle. Due better utilization of exergy, the exergy efficiency is maximum at that range. For recompression cycle, Exergy loss is almost constant with very small variation. But the exergy efficiency changes by 3.5-4% within the pressure range.

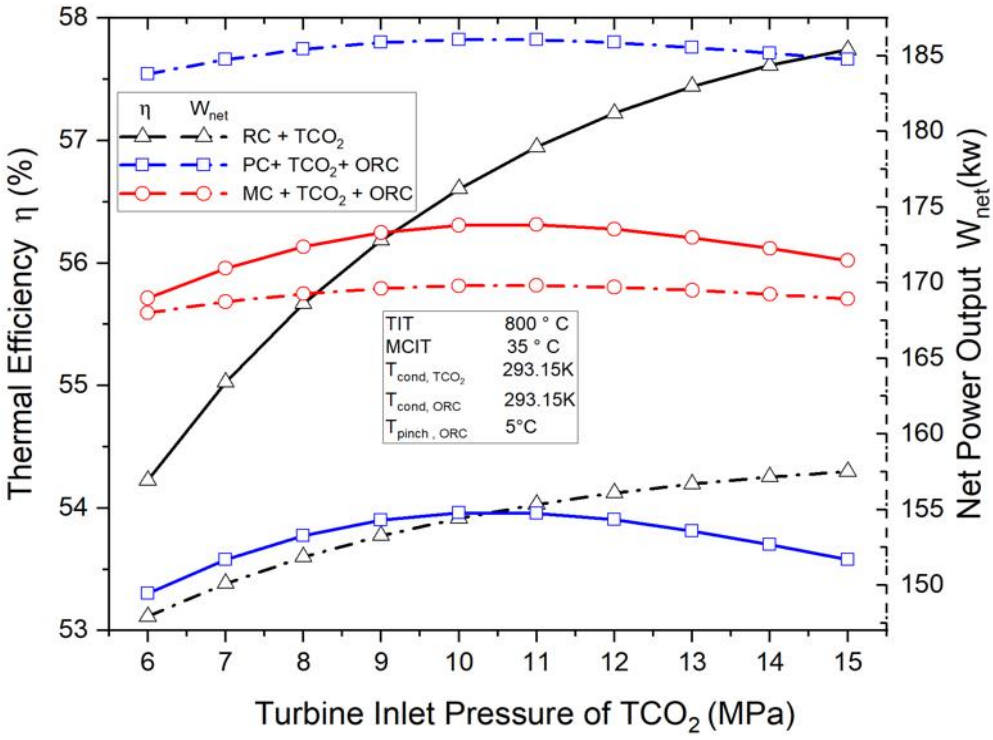

(a) Energy efficiency vs T-CO_2 turbine inlet pressure (MPa)

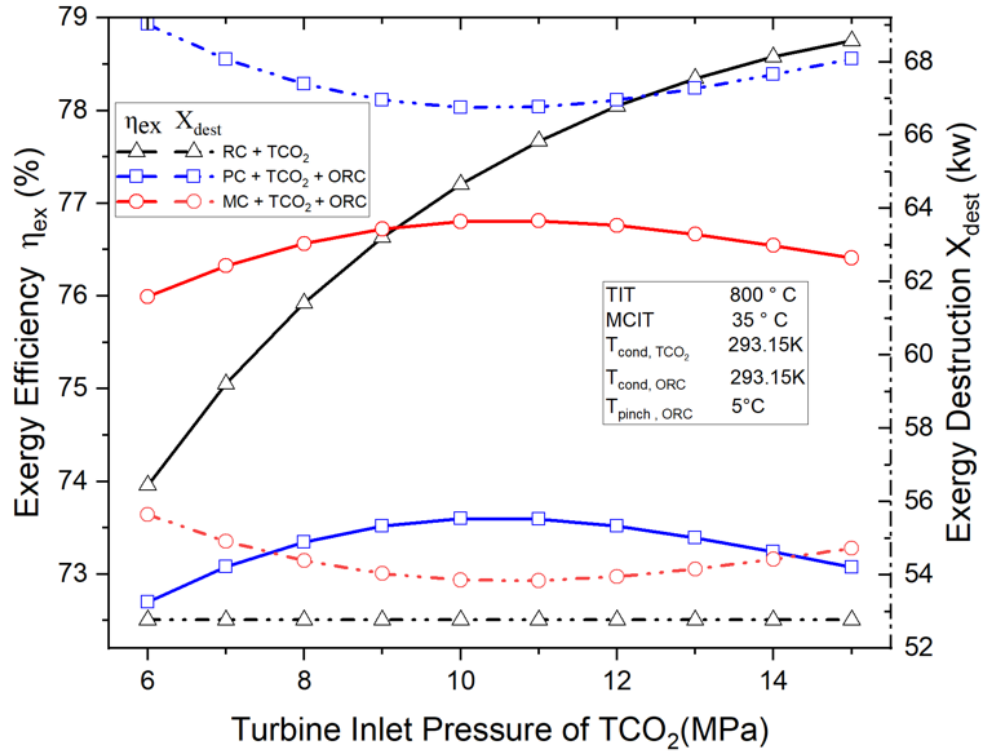

(b)Exergy efficiency vs T-CO_2 turbine inlet pressure (MPa)

Fig 15: Analysis of combined SCO_2 TCO_2 ORC configurations using Turbine Inlet Pressure of TCO_2

5.5 Impact of TCO_2 pressure ratio:

In this section, analysis has been done considering the pressure ratio of the TCO_2 cycle. In TCO_2 cycle, the lower pressure is the condensation pressure which is to be adjusted considering the fact that the saturation temperature corresponding to that pressure is appropriate to reject waste heat to the external environment. For this reason, keeping the condensation pressure constant, the upper pressure of TCO_2 cycle is varied which causes change in pressure ratio of the bottoming TCO_2 cycle. Since only the upper pressure is varied, so the variations in each of the parameters is exactly same as that of the previous section, only here pressure ratio is chosen as independent variable instead of TCO_2 cycle. Fig 16a shows that the maximum thermal efficiency for combined partial cooling and main compression cycle can be achieved at 1.7 – 1.9 pressure ratio of the TCO_2 cycle. Among the 3 cycles, maximum power output of 58.7 kw can be obtained at the combined partial cooling cycle model at pressure ratio of 1.8.

Similarly, in case of exergy Fig 16(b) the destruction is minimum when the pressure ratio lies within the range 1.75-1.9. For combined recompression cycle, exergy destruction decreases slightly but the change is negligible.

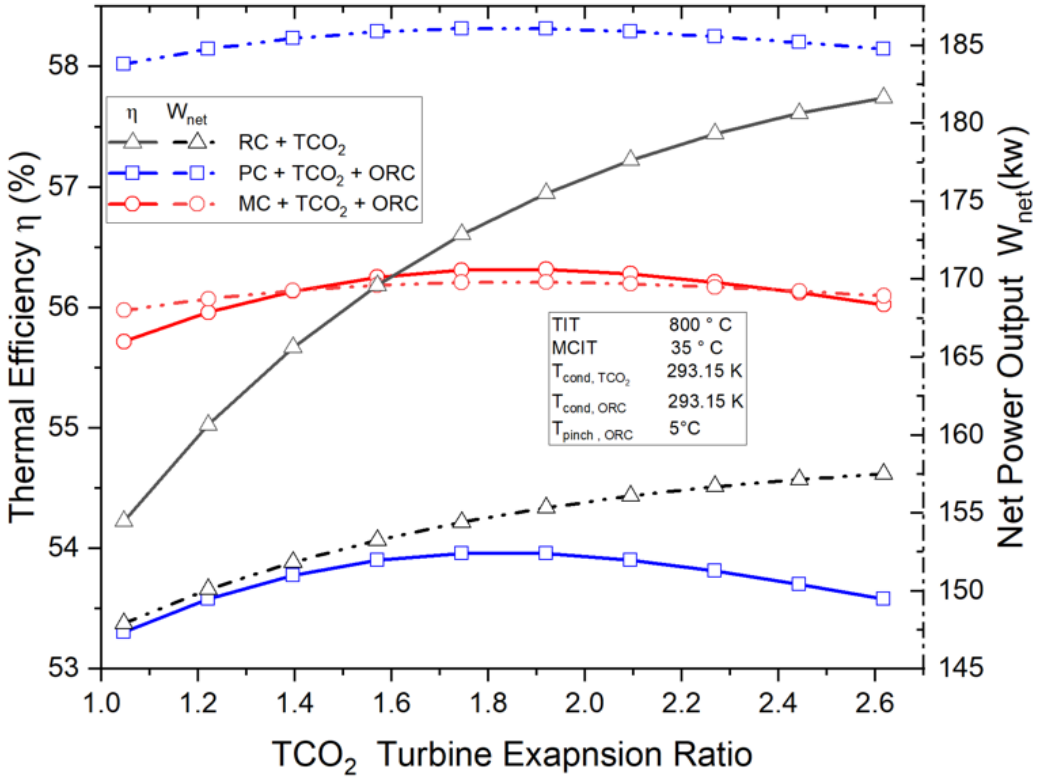

(a) Energy efficiency vs T-CO_2 Pressure Ratio (MPa)

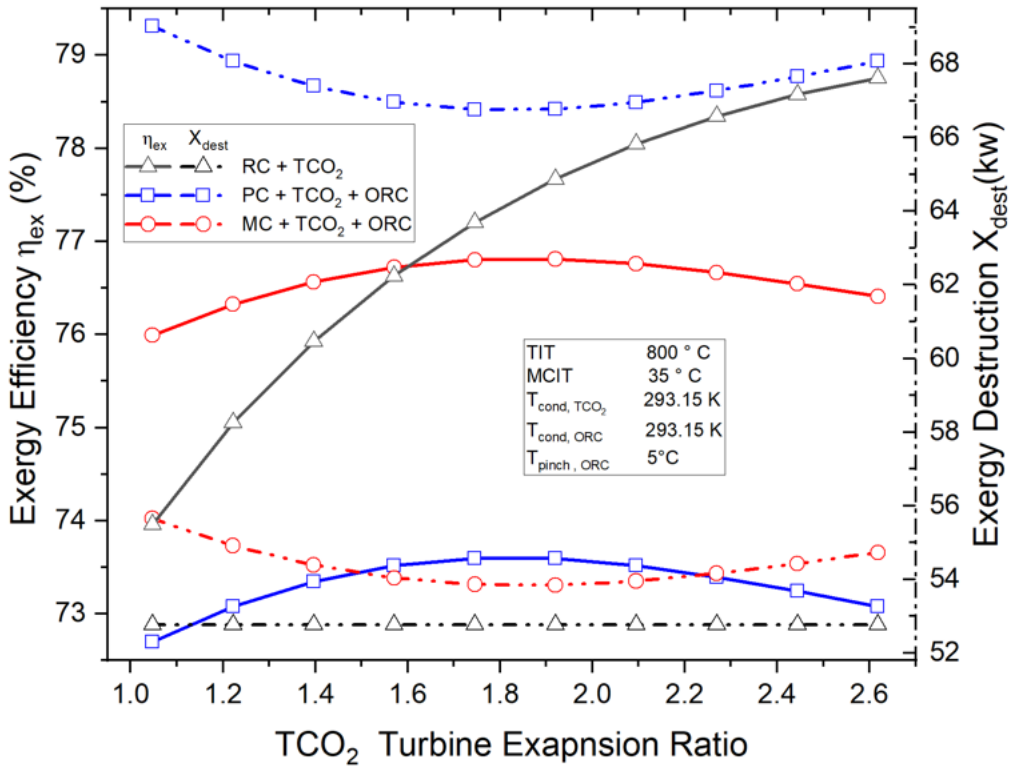

(b) Exergy efficiency vs T-CO_2 Pressure Ratio (MPa)

Fig 16: Analysis of combined SCO_2 TCO_2 ORC configurations using Pressure ratio of TCO_2 cycle

5.6 <u>Impact of Condensation Temperature of TCO_2 cycle:</u>

In T-CO_2 cycle, the lower pressure lies below the critical pressure. So, the state at point 1t i.e at the outlet of the condenser lies at subcritical state. This point is to be maintained at saturated liquid point corresponding to the lower pressure of the T-CO_2 cycle. Since, the state is saturated liquid state, in order to vary the condensation temperature, corresponding lower pressure of the TCO_2 cycle is to be varied. Fig 17a and 17b includes the result of the analysis done with the variation of this saturated temperature. It can be seen that the performance of each of the models declines almost linearly with the rise in condensation temperature. Lower condensation pressure causes higher pressure ratio of T-CO_2 cycle which results in more expansion inside turbine generating more output work. Figure 17 reflects that lower condensation temperature gives better performance in terms of both thermal and exergy efficiency. Along with efficiency, net output work generated also lessens. So, condensation temperature is to be kept lower as possible. But the limitation is that, heat from the condenser is rejected to the external environment, for which condensation

temperature must be equal to or greater than ambient temperature. In order to operate at below ambient temperature, additional refrigeration or cooling system is to be used to carry the rejected heat. It will require high cost, more complexity, maintenance etc. Figure 17 shows that the combined recompression cycle model gives best performance at very low condensation temperature upto 21 °C. At temperature higher than 21°C, combined main compression cycle gives better performance than recompression one. The partial cooling cycle gives 1.5–2 % less efficiency than recompression one. The variation in net power output is very small compared to the thermal efficiency. Net power output and exergy destruction is maximum for combined partial cooling cycle model. Because of the layout of the partial cooling cycle model, its power input and output is higher but efficiency is lesser in comparison to other cycle models. The change in exergy loss is negligible for all 3 models (Fig 17b). For partial cooling cycle, the change in exergy destruction is greater than other 2 models.

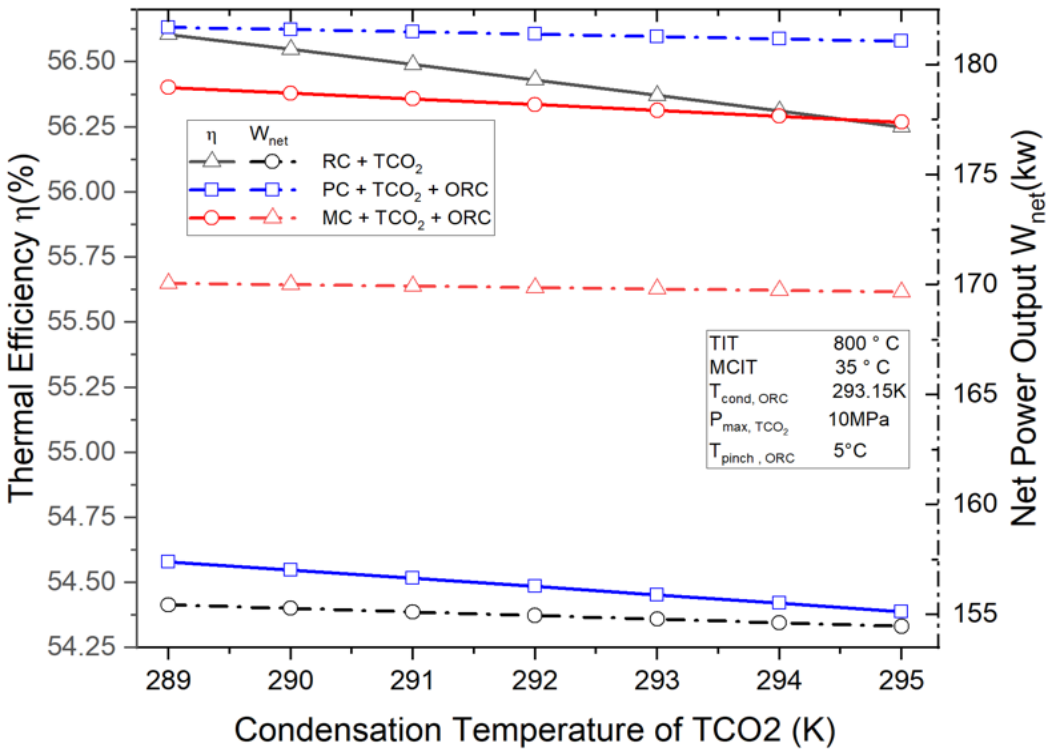

(a) Energy efficiency vs Condensation temperature of TCO_2 cycle

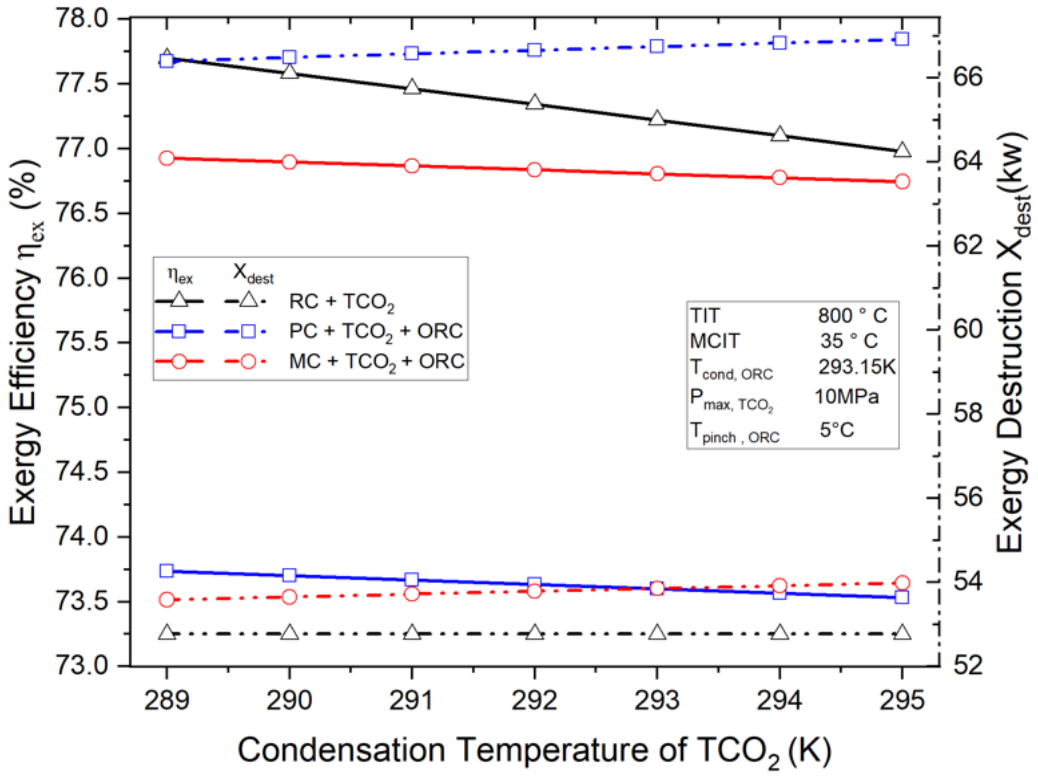

(b) Exergy efficiency vs Condensation Temperature of TCO_2 cycle

Fig 17: Analysis of combined SCO_2 TCO_2 ORC configurations using Condensation Temperature of TCO_2 cycle

5.7 Impact of ORC pinch temperature:

The ORC cycle layout is quite different from the TCO_2 cycle layout. ORC cycle is simple Rankine Cycle. As dry refrigerants are used, the state at outlet of heat recovery is saturated vapour state. This state must be located below the critical point of the refrigerant. During the expansion process inside the turbine, refrigerant always remains in the superheated state vapour, no phase change occurs during energy extraction from fluid. As the turbine inlet point lies at saturated vapour state below critical point, the pinch point has significant impact on the performance of ORC. Lower pinch temperature involves higher temperature at the turbine inlet causing more heat transfer to the bottoming cycle which generates higher work output in the bottoming cycle. As a result, there is increase in pressure ratio in the ORC cycle. The turbine generates more work by expanding more. Figure18a denotes the linear reduction in thermal efficiency and net power output with the rise of pinch temperature. Figure 18b shows that exergy loss increases with the rise in pinch

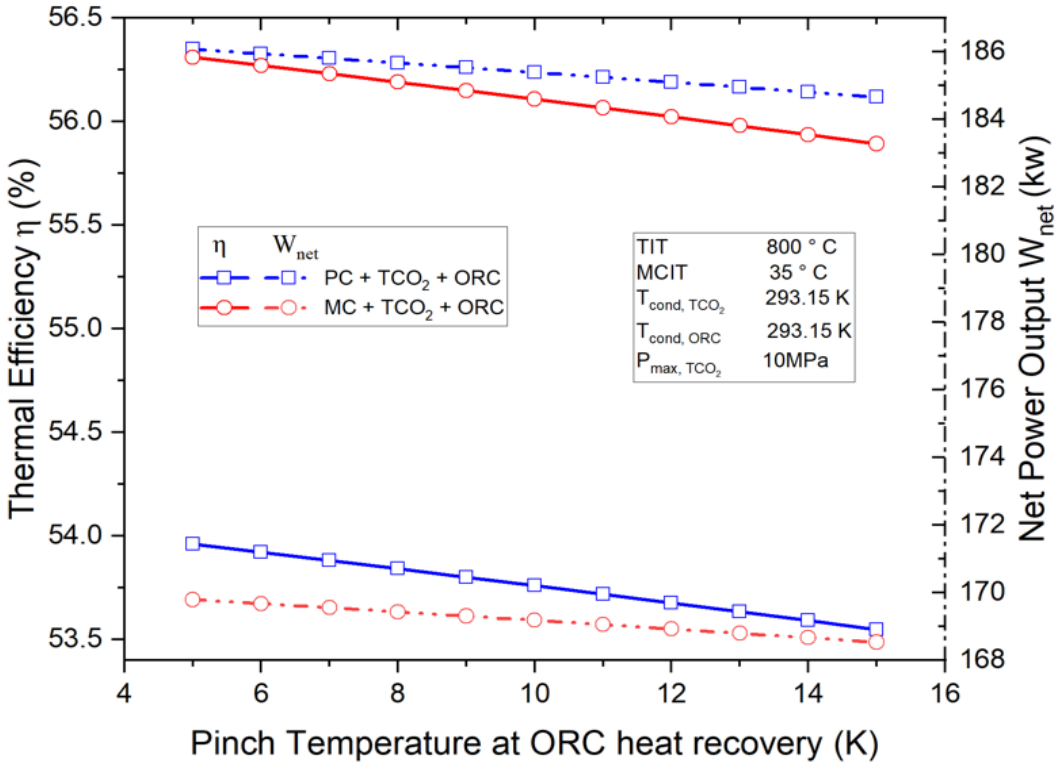

(a) Energy efficiency vs Pinch Temperature at heat recovery II

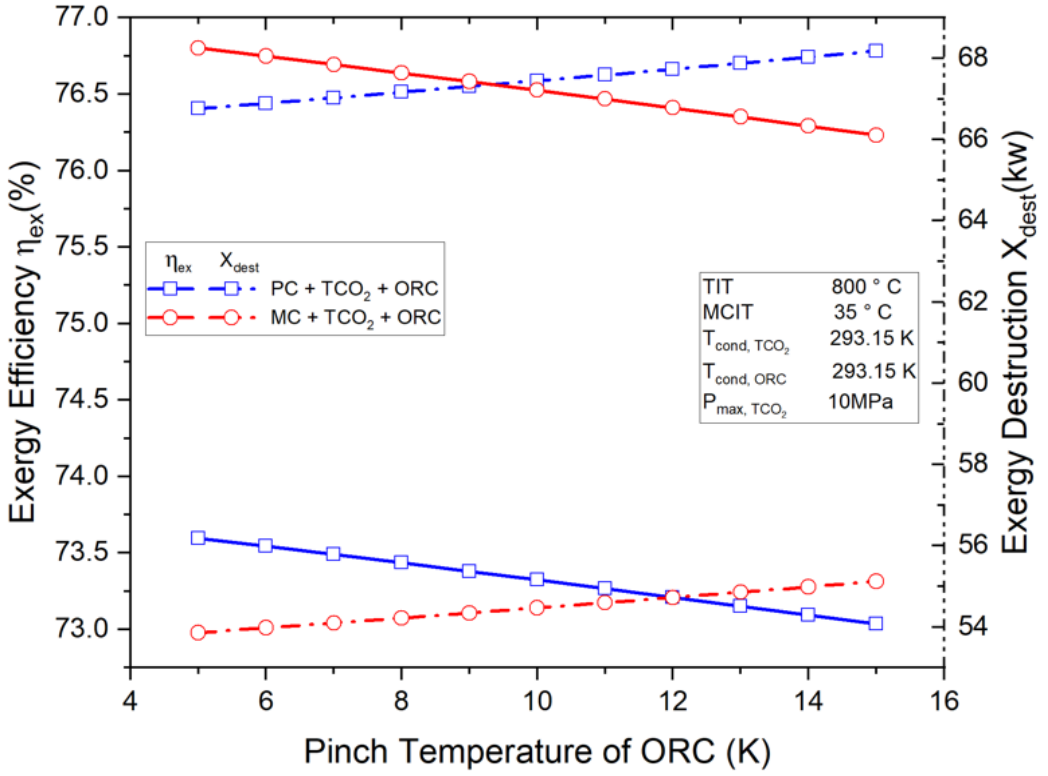

(b) Exergy efficiency vs Pinch Temperature Pinch Temperature at heat recovery II

Fig 18: Analysis of combined SCO_2 TCO_2 ORC configurations using Pinch Temperature heat recovery II

Temperature resulting in lower exergy efficiency. From these two graphs, we can see that the main compression cycle gives about 2.25% better performance than the partial cooling cycle in terms of thermal efficiency and 3- 3.5% in terms of exergy efficiency. Here combined recompression cycle is absent since that model has no ORC cycle.

5.8 Impact of pressure ratio of ORC:

As the point at the outlet of the heat recovery is saturated vapour, variation of pinch point causes variation in the maximum pressure of the ORC cycle. Lesser the pinch temperature, more is the maximum pressure. So, more work is obtained by the ORC cycle which causes improvement in overall efficiency of the combined cycle. The variation of cycle performance with respect to pressure ratio of ORC is shown in the figure 19a and 19b. More pinch temperature causes reduction in pressure ratio. Higher pressure ratio involves more turbine work which results in more work output and more thermal efficiency. As more work is obtained, exergy loss reduces and exergy efficiency increases. From fig 19a, it is clear that the thermal efficiency and net power output rises linearly with the rise in pressure ratio. Though the combined partial cooling cycle model generates 15-16 kw more output work, its efficiency is about 2.5% lesser than combined main compression cycle.

Figure 17b shows that significant variation in exergy loss occurs with the change in pressure ratio. At low pressure ratio, exergy loss is comparatively more and is linearly falls along with the increase in pressure ratio. Exergy efficiency of main compression cycle is approximately 3% higher than partial cooling cycle at constant particular ratio

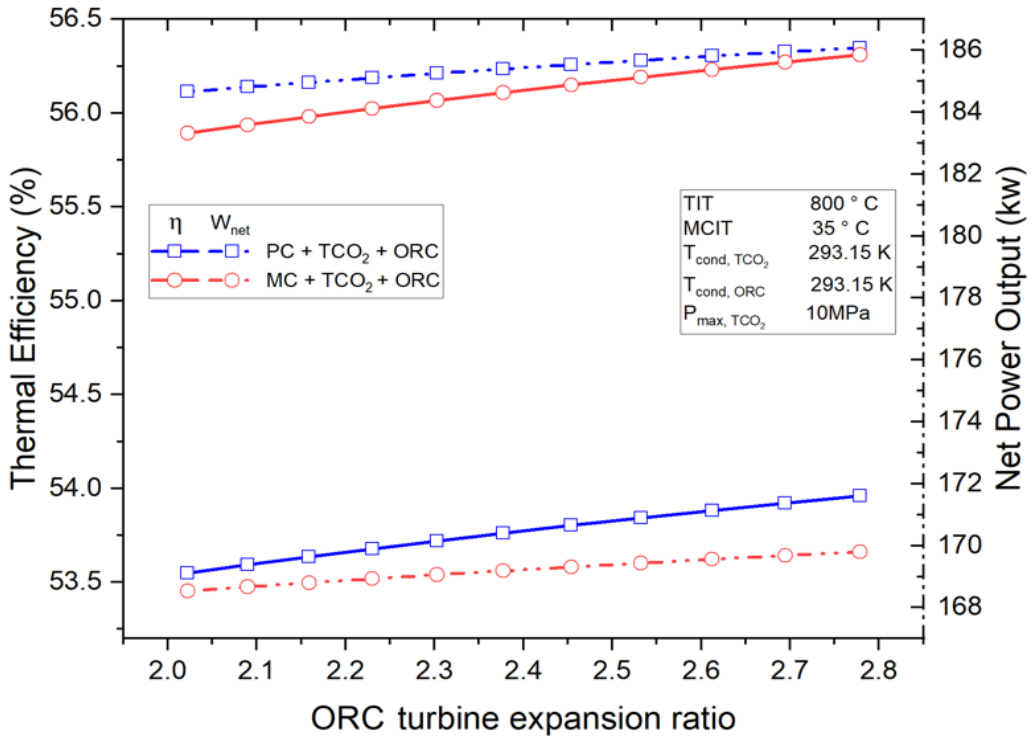

(a) Energy efficiency vs ORC pressure ratio

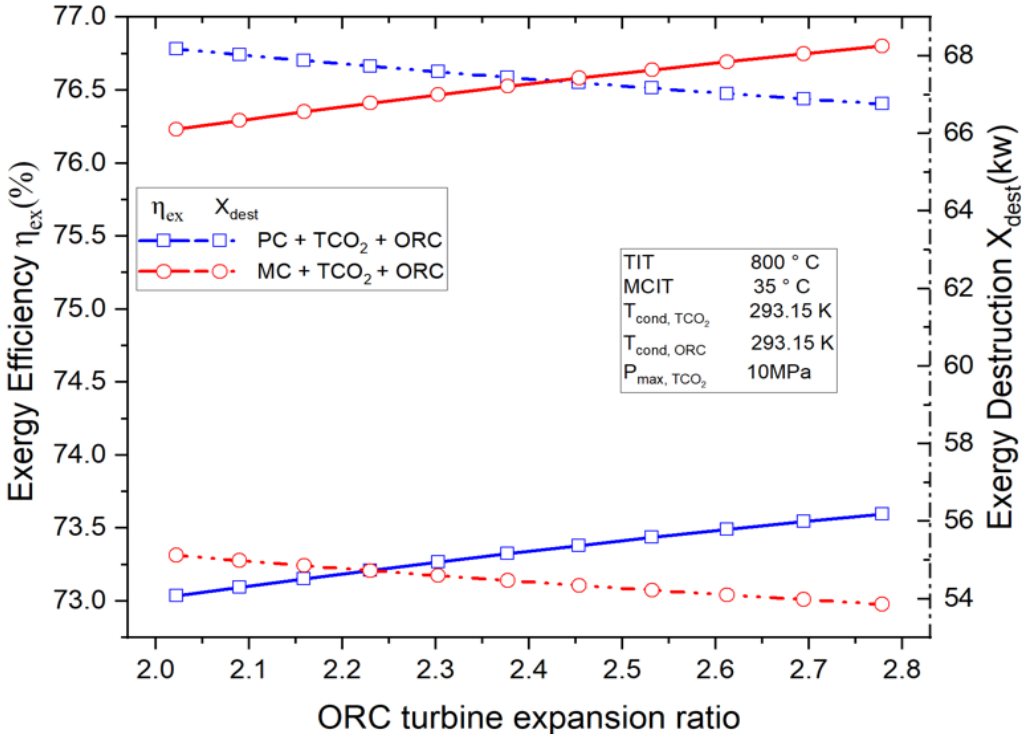

(b) Exergy efficiency vs ORC pressure ratio

Fig 19: Analysis of combined SCO_2 TCO_2 ORC configurations using ORC pressure ratio

5.9 Impact of Condensation Temperature of ORC:

The effect of condensation temperature of ORC cycle has the similar effect as that of the T-CO_2. Low condensation pressure causes high pressure ratio in the ORC cycle, resulting in a greater expansion inside the turbine and an increase in output work. Figure 20 demonstrates that reduced condensation temperatures result in greater thermal and exergy efficiency. Alongside reduction in efficacy, the amount of net output work falls. Similar type of variation can be observed in case of exergy. Therefore, the condensation temperature should be kept as low as feasible. However, since the condenser rejects heat to the external environment, condensation temperature must be equal to or greater than ambient temperature. To operate at temperatures below the ambient temperature, additional refrigeration or chilling systems are required to transport the rejected heat. It will necessitate high costs, increased complexity, upkeep, etc. It is to be mentioned that the change in thermal efficiency is not significant, only 0.1-0.2% within the given range. For net power output, variation is less 1 kw. Similarly for exergy efficiency, only 0.3 - 0.4% change can be observed for condensation temperature 16 to 22°C. Exergy loss increases by 1 -1.3 kw with the rise in condensation temperature resulting in exergy efficiency to lessen.

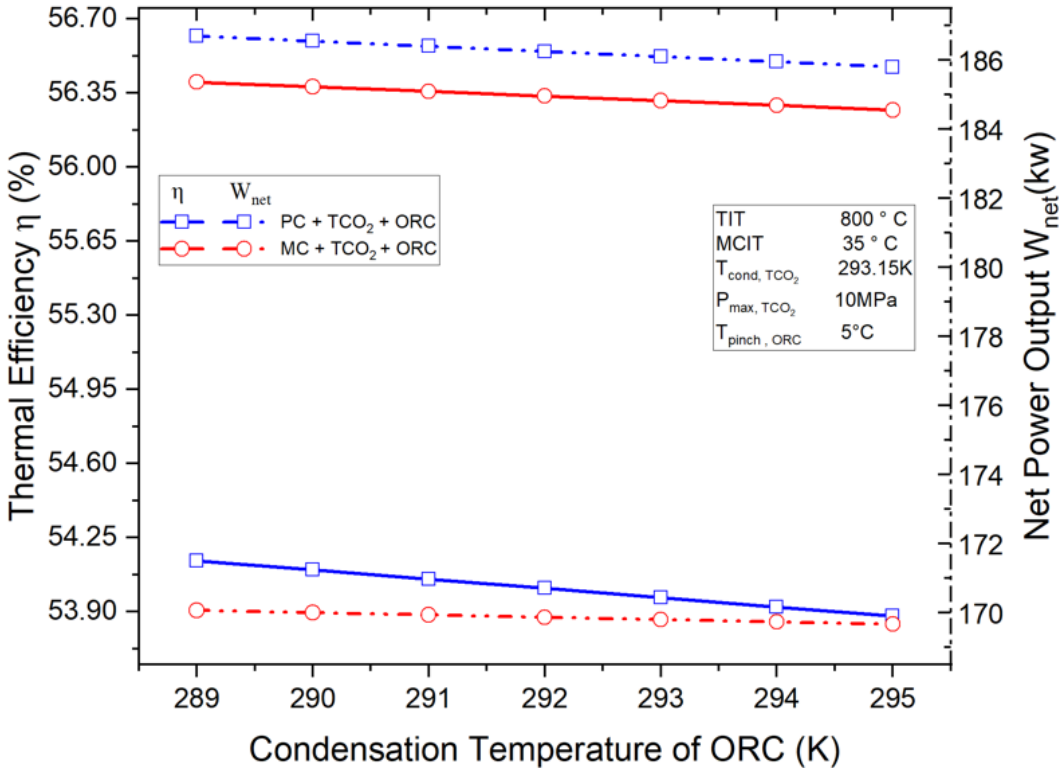

(a)Energy efficiency vs condensation temp of ORC

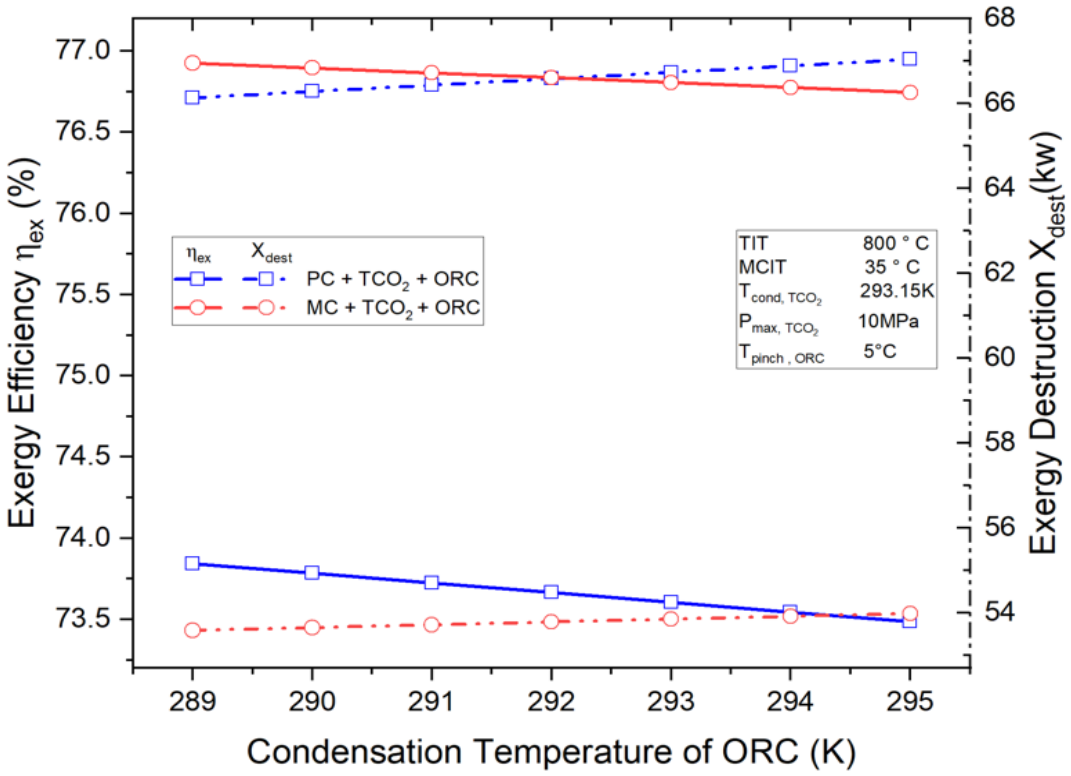

(b) Exergy efficiency vs Condensation temp of ORC

Fig 20: Analysis of combined SCO_2 TCO_2 ORC configurations using condensation temp of ORC

5.10 *Impact of various Refrigerants:*

Now let us see the different types refrigerants that can be used in the ORC cycle. Refrigerant is chosen considering factors like performance, green house impact, material effect etc. The organic fluids environmental effects must also be considered. Principal matters are the potential for ozone depletion, global warming etc. Some working fluids, such as R-11 and R-115, have already been phased out, while others, such as R141b and R142b, will be banned in the near future. This study does not consider these working fluids. Despite the fact that many of the working substances under consideration are flammable, they can be handed with proper precautions. Furthermore, auto-ignition is not a concern in this investigation because ORC cycles are operated at relatively low temperature. Besides, the fluid is unstable at temperatures near to its critical point; so an adequate difference is required between the maximum temperature limit of the cycle and the critical temperature. However, literature does not provide a singular interpretation of the reasonable distance. Proposal of Rayegan and Tao is utilized in this paper. In this method, the cycle's

maximum temperature is limited to a point on the saturation curve where the slope of the T-s diagram is infinite. The temperature is further raised to a point where further temperature increases cause working fluid's quality to decline below 99.9% during the expansion process. Notable is the fact that presuming 99% dryness is unnecessary and the cycle can successfully generate power with lower dryness. However, reducing this value to 90% has little effect on efficacy. Considering all the factors, R236ea, R245fa, butane and some other refrigerants are shortlisted for further consideration.

In figure 21a and 21b, comparison of various environmentally friendly refrigerants is shown in terms of both thermal and exergy for combined cycles both the cycles.

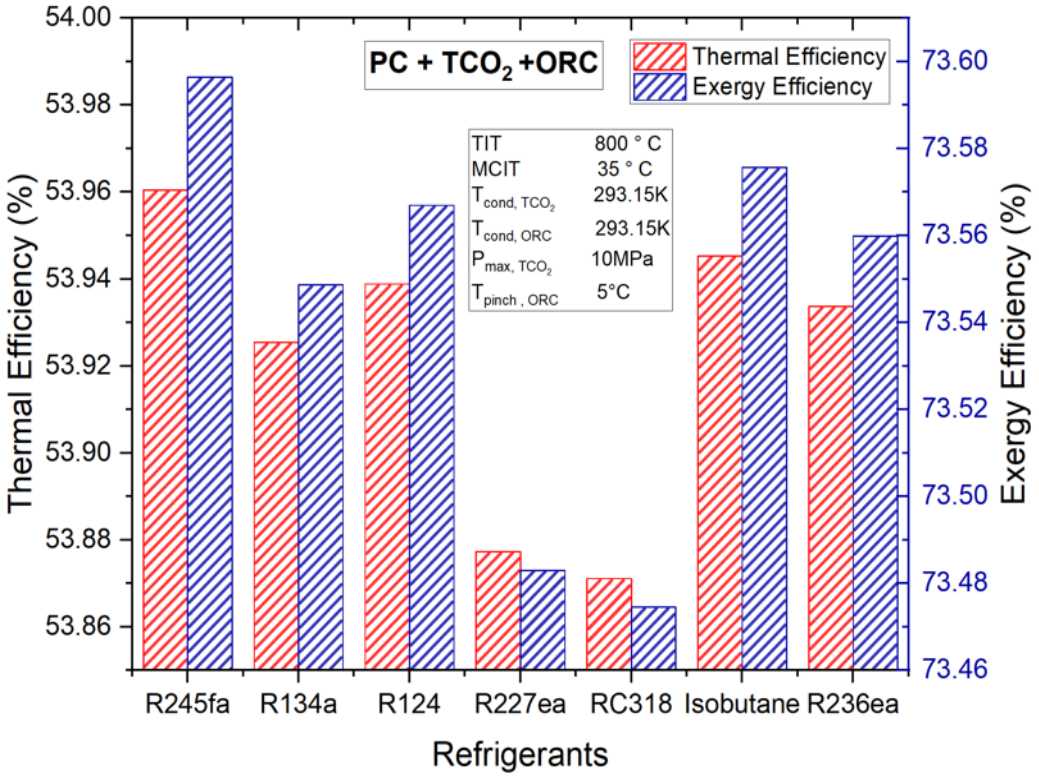

(a) Combined partial cooling SCO_2 TCO_2 ORC

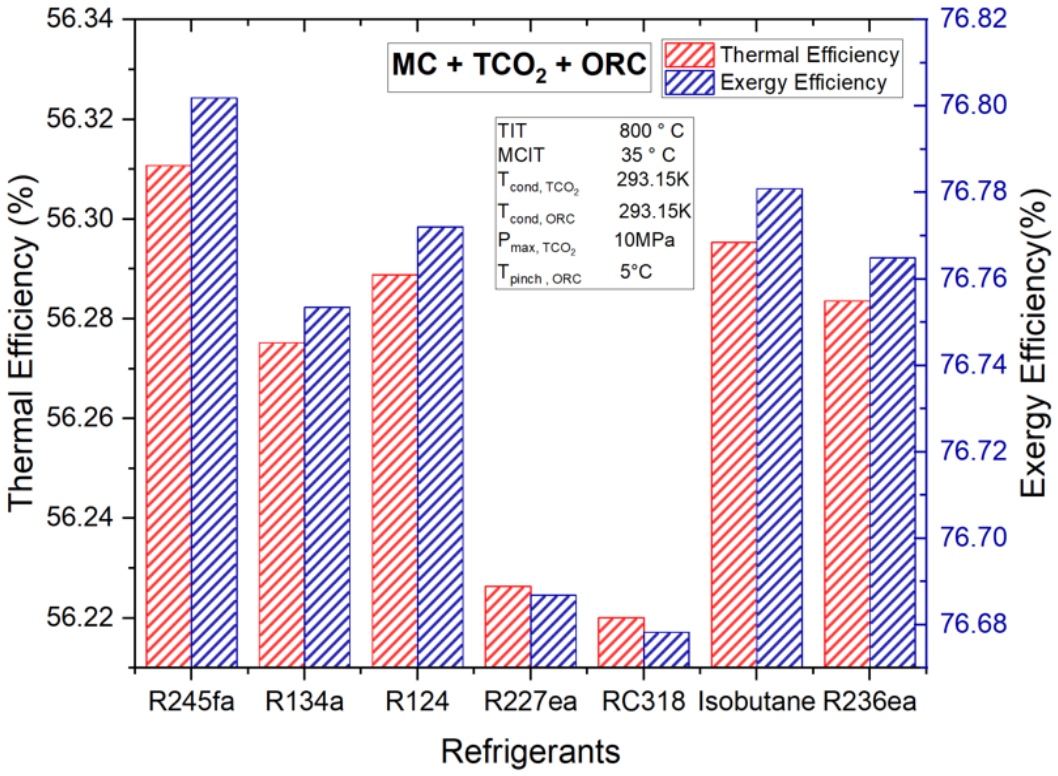

(b) Combined main compression SCO_2 TCO_2 ORC

Fig 21: Analysis of combined SCO_2 TCO_2 ORC configurations using various refrigerants

From these two figures, we see that R245fa refrigerants gives the best performance among the suitable refrigerants selected. Besides, R245fa is environmentally friendly and non-flammable, which are important issues that needs to be considered in working fluid selection. For these reasons, throughout the study we have used R245fa for the parametric analysis.

Chapter 6

Conclusion and Future work

In this paper we worked with S-CO_2 merged with T-CO_2 cycle and ORC cycle. In this paper, 3 different layouts of topping SCO_2, the study we have found that combined main compression cycle gives better performance than other cycle combinations. On the other hand, partial cooling cycle gives lesser efficiency compared to other cycles. Through validating and parametric analysis, we came to know that the thermal and exergy efficiency progress with the increase of maximum cycle temperature. In contrast, both efficiencies decrease due to increase in compressor inlet temperature of the bottoming cycle, only some increase in the efficiency can be observed near the critical point because of pseudocritical effects. But in case of turbine inlet pressure of the TCO_2 cycle, the efficiencies increase up to a certain value and then starts declining. Condensation Temperature has similar kind of impact on both the bottoming cycles. The condensation temperature has to be kept as minimum as possible according to the ambient temperature. At the recuperator, lower pinch temperature gives better performance. Throughout the study, the maximum temperature of the topping cycle was taken 800°C, compressor inlet temperature as 35°C, maximum pressure as 25MPa, condensation temperature at 293.15K. The combined cycle showed comparatively much better performance than standalone cycle for each of the 3 proposed models.

On this topic, further research can be done on following cases:

1. The model of T-CO_2 cycle can be modified to improve its thermal and exergy efficiency
2. Instead of using single stage turbine, multistage turbine with reheater can be used in topping and bottoming cycles
3. Multistage compressor with intercooler can be used at the place of main compressor and the rejected heat can be utilized for other purposes.
4. Cogeneration plant can be integrated with the cycle to utilize the waste heat
5. Open feedwater and closed feedwater heaters can be used for further improvement
6. Nanofluids and other kinds of fluids which have better heat absorbtivity, high specific heat can be used.

References

[1] A. W. Dowling, T. Zheng, and V. M. Zavala, "Economic assessment of concentrated solar power technologies: A review," *Renewable and Sustainable Energy Reviews*, vol. 72. Elsevier Ltd, pp. 1019–1032, 2017. doi: 10.1016/j.rser.2017.01.006.

[2] M. J. Li, H. H. Zhu, J. Q. Guo, K. Wang, and W. Q. Tao, "The development technology and applications of supercritical CO2 power cycle in nuclear energy, solar energy and other energy industries," *Applied Thermal Engineering*, vol. 126. Elsevier Ltd, pp. 255–275, 2017. doi: 10.1016/j.applthermaleng.2017.07.173.

[3] S. Duniam, I. Jahn, K. Hooman, Y. Lu, and A. Veeraragavan, "Comparison of direct and indirect natural draft dry cooling tower cooling of the sCO2 Brayton cycle for concentrated solar power plants," *Appl Therm Eng*, vol. 130, pp. 1070–1080, Feb. 2018, doi: 10.1016/j.applthermaleng.2017.10.169.

[4] "The Supercritical Thermodynamic Power Cycle," Fergamon Pre~s, 1968.

[5] "Garg P, Srinivasan K, Dutta P, Kumar P. Comparison of CO2 and steam in transcritical Rankine cycles for concentrated solar power. Energy Procedia 2014;49:1138–46.".

[6] "Persichilli M, Kacludis A, Zdankiewicz E, Held T. Supercritical CO2 power cycle developments and commercialization: why sCO2 can displace steam ste. Power-Gen".

[7] "Cheng L. Evaluation of Correlations for Supercritical CO2 Cooling Convective Heat Transfer and Pressure Drop in Macro-and Micro-Scale Tubes. Int J Microsc Nanosc Therm Fluid Transp Phenom 2014;5(2):113.".

[8] "Ehsan MM, Guan Z, Klimenko A. A comprehensive review on heat transfer and pressure drop characteristics and correlations with supercritical CO 2 under heating and cooling applications. Renew Sustain Energy Rev 2018;92:658–75.".

[9] "Feher, E. G., 'The Supercritical Thermodynamic Power Cycle', Advances in Energy Conversion Engineering, August 13-17, Intersociety Energy Conversion Engineering Conference, New York, American Society of Mechanical Engineers, 1967".

[10] "Dostal V, Hejzlar P, Driscoll MJ. High-performance supercritical carbon dioxide cycle for next-generation nuclear reactors. Nucl Technol 2006;154(3):265e82.".

[11] "Neises T, Turchi C. A comparison of supercritical carbon dioxide power cycle configurations with an emphasis on CSP applications. Energy Procedia 2014;49:1187e96.".

[12] "Ma Z, Turchi CS. Advanced supercritical carbon dioxide power cycle configurations for use in concentrating solar power systems: preprint. Golden, CO: National Renewable Energy Laboratory (NREL); 2011.".

[13] "Cheng L. Evaluation of correlations for supercritical CO2 cooling convective heat transfer and pressure drop in macro-and micro-scale tubes. Int J Microscale Nanoscale Thermal Fluid Transport Phenomena 2014;5(2):113.".

[14] “Conboy T, Wright S, Pasch J, Fleming D, Rochau G, Fuller R. Performance characteristics of an operating supercritical CO2 Brayton cycle. J Eng Gas Turbines Power 2012;134(11):111703.”.

[15] “Ehsan MM, Guan Z, Klimenko A. A comprehensive review on heat transfer andpressure drop characteristics and correlations with supercritical CO 2 under heating and cooling applications. Renew Sustain Energy Rev 2018;92:658e75.”.

[16] “Xu J, Sun E, Li M, Liu H, Zhu B. Key issues and solution strategies for supercritical carbon dioxide coal fired power plant. Energy 2018;157:227e46.”.

[17] “Ma, Z., and Turchi, C., 2011, ‘Advanced Supercritical Carbon Dioxide Power Cycle Configurations for Use in Concentrating Solar Power Systems,’ Proceedings of Supercritical CO2 Power Cycle Symposium 2011, Boulder, CO, May 24–25.”.

[18] C. , M. Z. , and D. Turchi, “Turchi, C., Ma, Z., and Dyreby, J., 2012, ‘Supercritical CO2 for Application in Concentrating Solar Power Systems,’ Proceedings of ASME Turbo Expo 2012, Copenhagen, Denmark, June 11–15.”.

[19] M. M. Ehsan, Z. Guan, and A. Y. Klimenko, “A comprehensive review on heat transfer and pressure drop characteristics and correlations with supercritical CO2 under heating and cooling applications,” *Renewable and Sustainable Energy Reviews*, vol. 92. Elsevier Ltd, pp. 658–675, Sep. 01, 2018. doi: 10.1016/j.rser.2018.04.106.

[20] C. S. Turchi, Z. Ma, T. W. Neises, and M. J. Wagner, “Thermodynamic study of advanced supercritical carbon dioxide power cycles for concentrating solar power systems,” *Journal of Solar Energy Engineering, Transactions of the ASME*, vol. 135, no. 4, 2013, doi: 10.1115/1.4024030.

[21] “Dostal V., Driscoll M. J., Hejzlar P., and Todreas N. E., 2002. ‘A supercritical CO2 gas turbine power cycle for nextgeneration nuclear reactors’. In 10th International Conference on Nuclear Engineering, Arlington, Virginia, 2002, ASME Paper ICONE10-22192.”.

[22] “Dostal V., 2004. ‘A supercritical carbon dioxide cycle for next generation nuclear reactors’. Ph.D. Thesis, Massachusetts Institute of Technology, USA.”.

[23] “Hejzlar P., Dostal V., Driscoll M. J., Dumaz P., Poullennec G., and Alpy N., 2006. ‘Assessment of gas cooled fast reactor with indirect supercritical CO2 cycle’. Nuclear Engineering and Technology, 38, pp. 109-118.”.

[24] “Besarati SM, Goswami DY. Analysis of advanced supercritical carbon dioxide power cycles with a bottoming cycle for concentrating solar power applications. J Sol Energy Eng 2014;136(1):010904.”.

[25] “Kim S, Cho Y, Kim MS, Kim M. Characteristics and optimization of supercritical CO2 recompression power cycle and the influence of pinch point temperature difference of recuperators. Energy 2018;147:1216–26.”.

[26] “Dyreby J, Klein S, Nellis G, Reindl D. Design considerations for supercritical carbon dioxide Brayton cycles with recompression. J Eng Gas Turbines Power 2014;136(10):101”.

[27] “Padilla RV, Too YCS, Benito R, Stein W. Exergetic analysis of supercritical CO 2 Brayton cycles integrated with solar central receivers. Appl Energy 2015;148:348–65.”.

[28] “Padilla RV, Too YCS, Beath A, McNaughton R, Stein W. Effect of pressure drop and reheating on thermal and exergetic performance of supercritical carbon dioxide Brayton cycles integrated with a solar central receiver. J Sol Energy Eng 2015;137(5):051012.”.

[29] “Wang J. F., Sun Z. X., Dai Y. P., and Ma S. L., 2010. ‘Parametric optimization design for supercritical CO2 power cycle using genetic algorithm and artificial neural network’. Applied Energy, 87, pp. 1317-1324.”.

[30] “Song Y. H., Wang J. F., Dai Y. P., and Zhou E. M., 2012. ‘Thermodynamic analysis of a transcritical CO2 power cycle driven by solar energy with liquified natural gas as its heat sink’. Applied Energy, 92, pp. 194-203.”.

[31] “Ishiyama S., Mutoa Y., Kato Y., Nishio S., Hayashi T., and Nomoto Y., 2008. ‘Study of steam, helium and supercritical CO2 turbine power generations in prototype fusion power reactor’. Progress in Nuclear Energy, 50, pp. 325-332.”.

[32] “Liu L, Gu C, Ren X. An investigation of the conjugate heat transfer in an intercooled compressor vane based on a discontinuous galerkin method. Appl Therm Eng 2017;114:85e97.”.

[33] “Zhang Q, Ogren R, Kong S. Thermo-economic analysis and multi-objective optimization of a novel waste heat recovery system with a transcritical CO2 cycle for offshore gas turbine application. Energy Convers Manag 2018;172: 212e27.”.

[34] S. M. Besarati and D. Y. Goswami, “Analysis of Advanced Supercritical Carbon Dioxide Power Cycles With a Bottoming Cycle for Concentrating Solar Power Applications,” *Journal of Solar Energy Engineering, Transactions of the ASME*, vol. 136, no. 1, Feb. 2014, doi: 10.1115/1.4025700.

[35] “Song J, Song Y, Gu C. Thermodynamic analysis and performance optimization of an Organic Rankine Cycle (ORC) waste heat recovery system for marine diesel engines. Energy 2015;82:976e85.”.

[36] “Persichilli M, Kacludis A, Zdankiewicz E, Held T. Supercritical CO2 power cycle developments and commercialization: why S-CO2 can displace steam. Power- Gen India and Central Asia; 2012.”.

[37] “Marchionni M, Bianchi G, Tsamos KM, Tassou SA. Techno-economic comparison of different cycle architectures for high temperature waste heat to power conversion systems using CO 2 in supercritical phase. Energy Procedia 2017;123:305–12.”.

[38] “Chen Y. Novel cycles using carbon dioxide as working fluid (Licentiate thesis). Stockholm, Sweden: School of Industrial Engineering and Management; 2006.”.

[39] “Hung, T. C., Shai, T. Y., Wang, S. K., 1997, ‘A Review of Organic Rankie Cycles (ORCs) for the Recovery of Low-Grade Waste Heat,’ Energy, 22(7), pp. 661–667.”.

[40] “Quoilin S, Van Den Broek M, Declaye S, Declaye S, Dewallef P, Lemort V. Techno-economic survey of organic rankine cycle (ORC) systems. Renew Sust Energ Rev 2013;22:168e86.”.

[41] “Lecompte S, Huisseune H, van den Broek M, Vanslambrouck B, De Paepe M. Review of organic Rankine cycle (ORC) architectures for waste heat recovery. Renew Sust Energ Rev 2015;47:448e61.”.

[42] “Ayachi F, Ksayer EB, Zoughaib A, Neveu P. ORC optimization for medium grade heat recovery. Energy 2014;68:47e56.”.

[43] “Lion S, Michos CN, Vlaskos I, Rouaud C, Taccani R. A review of waste heat recovery and Organic Rankine Cycles (ORC) in on-off highway vehicle Heavy Duty Diesel Engine applications. Renew Sust Energ Rev 2017;79:691e708”.

[44] “Sun W, Yue X, Wang Y. Exergy efficiency analysis of ORC (Organic Rankine Cycle) and ORC-based combined cycles driven by low-temperature waste heat. Energy Convers Manage 2017;135:63e73.”.

[45] “Eyidogan M, Kilic FC, Kaya D, Coban V, Cagman S. Investigation of Organic Rankine Cycle (ORC) technologies in Turkey from the technical and economic point of view. Renew Sust Energ Rev 2016;58:885e95”.

[46] “Yu GP, Shu GQ, Tian H, Wei HQ, Liu LN. Simulation and thermodynamic analysis of a bottoming Organic Rankine Cycle (ORC) of diesel engine (DE). Energy 2013;51:281e90.”.

[47] “Yue C, Han D, Pu WH. Analysis of the integrated characteristics of the CPS (combined power system) of a bottoming organic Rankine cycle and a diesel engine. Energy 2014;72:739e51.”.

[48] “Clemente S, Micheli D, Reini M, Taccani R. Bottoming organic Rankine cycle for a small scale gas turbine: a comparison of different solutions. Appl Energ 2013;106:355e64.”.

[49] “Mohammadi A, Kasaeian A, Pourfayaz F, et al. Thermodynamic analysis of a combined gas turbine, ORC cycle and absorption refrigeration for a CCHP system[J]. Appl Therm Eng 2017;111:397e406.”.

[50] “Song J, Gu CW. Performance analysis of a dual-loop organic Rankine cycle (ORC) system with wet steam expansion for engine waste heat recovery. Appl Energ 2015;156:280e9.”.

[51] “Perez-Pichel GD, Linares JI, Herranz LE, Moratilla BY. Thermal analysis of supercritical CO 2 power cycles: assessment of their suitability to the forthcoming sodium fast reactors. Nucl Eng Des 2012;250:23e34.”.

[52] “Chacartegui R, De Escalona JMM, Sanchez D, et al. Alternative cycles based on carbon dioxide for central receiver solar power plants[J]. Appl Therm Eng 2011;31(5):872e9.”.

[53] “Sanchez D, Brenes BM, Mu~noz de Escalona JM, Chacartegui R. Non-conventional combined cycle for intermediate temperature systems. Int J Energ Res 2013;37(5):403e11.”.

[54] “Besarati SM, Goswami DY. Analysis of advanced supercritical carbon dioxide power cycles with a bottoming cycle for concentrating solar power applications. J Sol Energ-T ASME 2014;136(1), 010904.”.

[55] “Zhang HZ, Shao S, Zhao H, Feng ZP. Thermodynamic analysis of a SCO2 partflow cycle combined with an organic Rankine cycle with liquefied natural gas as heat sink. In: ASME turbo expo 2014: turbine technical conference and exposition; 2014. V03BT36A012.”.

[56] “Chen, H., Goswami, D. Y., and Stefanakos, E. K., 2010, ‘A Review of Thermodynamic Cycles and Working Fluids for the Conversion of Low-Grade Heat,’ Renewable Sustainable Energy Rev., 14(9), pp. 3059–3067.”.

[57] “Chacartegui, R., Mu~ noz de Escalona, J. M., Sanchez, D., Monje, B., and Sanchez, T., 2011, ‘Alternative Cycles Based on Carbon Dioxide for Central Receiver Solar Power Plants,’ Appl. Therm. Eng., 31(5), pp. 872–879.”.

[58] “Sanchez, D., Brenes, B. M., de Escalona, J. M. M., and Chacartegui, R., 2012, ‘Non-Conventional Combined Cycle for Intermediate Temperature Systems,’ Int. J. Energy Res., 37(5), pp. 403–411.”.

[59] “Wright SA, Radel R, Conboy T, Rochau GE. Modeling and Experimental Results for Condensing Supercritical CO2 Power Cycles. Sandia Report 2011.”.

[60] “Wang, J. F., Sun, Z. X., Dai, Y. P., and Ma, S. L. (2010). ‘Parametric optimization design for supercritical CO2 power cycle using genetic algorithm and artificial neural network.’ Appl. Energy, 87(4), 1317–1324.”.

[61] “Wang, J. F., Zhao, P., Niu, X. Q., and Dai, Y. P. (2012). ‘Parametric analysis of a new combined cooling, heating and power system with transcritical CO2 driven by solar energy.’ Appl. Energy, 94, 58–64.”.

[62] “Song, Y. H., Wang, J. F., Dai, Y. P., and Zhou, E. M. (2012). ‘Thermodynamic analysis of a transcritical CO2 power cycle driven by solar energy with liquified natural gas as its heat sink.’ Appl. Energy, 92, 194–203.”.

[63] “Cao Y, Ren J, Sang Y, Dai Y. Thermodynamic analysis and optimization of a gas turbine and cascade CO2 combined cycle. Energy Convers Manage 2017;144:193–204.”.

[64] “Sarkar, J. (2009). ‘Second law analysis of supercritical CO2 recompression Brayton cycle.’ Energy, 34(9), 1172–1178.”.

[65] “Wang, X. R., Wu, Y., Wang, J. F., Dai, Y. P., and Xie, D. M. (2015). ‘Thermo-economic analysis of a recompression supercritical CO2 cycle combined with a transcritical CO2 cycle.’ Proc., ASME Turbo Expo, Montréal.”.

[66] “Chen, Y., Lundqvist, P., Johansson, A., and Platell, P. (2006). ‘A comparative study of the carbon dioxide transcritical power cycle compared with an organic Rankine cycle with R123 as working fluid in waste heat recovery.’ Appl. Therm. Eng., 26(17–18), 2142–2147.”.

[67] “Cayer, E., Galanisa, N., Desilets, M., Nesreddine, H., and Roy, P. (2009). ‘Analysis of a carbon dioxide transcritical power cycle using a low temperature source.’ Appl. Energy, 86(7–8), 1055–1063.”.

[68] “Cayer, E., Galanis, N., and Nesreddine, H. (2010). ‘Parametric study and optimization of a transcritical power cycle using a low temperature source.’ Appl. Energy, 87(4), 1349–1357.”.

[69] “Chen, Y., Lundqvist, P., Johansson, A., and Platell, P. (2006). ‘A comparative study of the carbon dioxide transcritical power cycle compared with an organic Rankine cycle with R123 as working fluid in waste heat recovery.’ Appl. Therm. Eng., 26(17–18), 2142–2147.”.

[70] C. S. Turchi, Z. Ma, T. W. Neises, and M. J. Wagner, “Thermodynamic study of advanced supercritical carbon dioxide power cycles for concentrating solar power systems,” *Journal of Solar Energy Engineering, Transactions of the ASME*, vol. 135, no. 4, 2013, doi: 10.1115/1.4024030.